Evaluation of a modified sequential P extraction protocol

Quantification of Fe(II)-P as a separate phase in seven different freshwater sediments

Haasler, Sina; Herzog, Simon David; O'Connell, David W.; Wisawapipat, Worachart; Wang, Qian; Hupfer, Michael; Papera de Oliveira, J.; Kragh, Theis; Klamt, Anna Marie; Reitzel, Kasper

DOI
10.1002/lom3.10716

Publication date
2025

Document Version
Final published version

Published in
Limnology and Oceanography: Methods

Citation (APA)
Haasler, S., Herzog, S. D., O'Connell, D. W., Wisawapipat, W., Wang, Q., Hupfer, M., Papera de Oliveira, J., Kragh, T., Klamt, A. M., & Reitzel, K. (2025). Evaluation of a modified sequential P extraction protocol: Quantification of Fe(II)-P as a separate phase in seven different freshwater sediments. *Limnology and Oceanography: Methods*, *23*(10), 765-784. https://doi.org/10.1002/lom3.10716

LIMNOLOGY
and
OCEANOGRAPHY: METHODS

ASLO

Limnol. Oceanogr.: Methods 23, 2025, 765–784

doi: 10.1002/lom3.10716

EVALUATIONS OF EXISTING METHODS

Evaluation of a modified sequential P extraction protocol: Quantification of Fe(II)-P as a separate phase in seven different freshwater sediments

Sina Haasler,[1] **Simon David Herzog**,[2] **David W. O'Connell**,[3] **Worachart Wisawapipat**,[4] **Qian Wang**,[5] **Michael Hupfer**,[6,7] **Jéssica Papera**,[8,9] **Theis Kragh**,[1] **Anna-Marie Klamt**,[1] **Kasper Reitzel**[1]*

[1]Department of Biology, Freshwater Ecology, University of Southern Denmark, Odense M, Denmark; [2]Department of Science and Environment, Roskilde University, Roskilde, Denmark; [3]Department of Civil, Structural & Environmental Engineering, Trinity College Dublin, The University of Dublin, Dublin 2, Ireland; [4]Department of Soil Science, Kasetsart University, Bangkok, Thailand; [5]Department of Environmental Science and Engineering, Guangdong Technion—Israel Institute of Technology, Shantou, Guangdong, China; [6]Department of Ecohydrology and Biogeochemistry, Leibniz-Institute of Freshwater Ecology and Inland Fisheries (IGB), Berlin, Germany; [7]Department of Aquatic Ecology, Brandenburg Technical University Cottbus-Senftenberg, Bad Saarow-Pieskow, Germany; [8]European Centre of Excellence for Sustainable Water Technology, Wetsus, Leeuwarden, The Netherlands; [9]Department of Biotechnology, Delft University of Technology, Delft, The Netherlands

Abstract

Sequential phosphorus (P) extraction (SPE) is a well-established and widely applied method for quantitatively and qualitatively determining the critical nutrient P in freshwater sediments. It allows the estimation of P bioavailability and facilitates the evaluation of the long-term effects of eutrophication mitigation measures. Most current protocols do not differentiate between redox-sensitive Fe(III)-P and more stable reduced Fe(II)-P minerals, such as vivianite. In this study, we tested a modified SPE protocol designed to quantify Fe(II)-P (vivianite-P) as a separate phase through the complexation of Fe(II) with 2,2′-bipyridine (Bipy). Seven lakes were selected as study sites with different sedimentary Fe and P contents and restoration histories. We validated the Bipy extraction step through direct comparison with results from the conventional protocol and the application of direct mineral detection methods, including x-ray absorption near-edge structure at the Fe and P K-edges, x-ray diffraction, optical microscopy, and scanning electron microscopy with energy dispersive x-ray spectroscopy. The Bipy fraction was primarily extracting P that was conventionally extracted in the bicarbonate-dithionite (redox-sensitive Fe/Mn-bound) and NaOH (metal-[Fe/Al-]bound) fractions. The results from the direct detection methods indicated that the extracted Fe(II)-P was predominantly vivianite. The efficiency of the Bipy extraction was decreased in samples with high crystallinity, but excessive Fe(II) or high organic content had minimal impact. Hence, it is highly recommended to use x-ray diffraction and x-ray absorption near edge structure in combination with the modified extraction protocol. Overall, the method tested with different freshwater sediments provides robust results when quantification of Fe(II)-P including vivianite is an important objective.

*Correspondence: reitzel@biology.sdu.dk

Associate editor: Ben Surridge

Data Availability Statement: Data are available via the public data repository Zenodo (https://doi.org/10.5281/zenodo.15018389).

Eutrophication of freshwater systems due to excessive nutrient inputs, primarily nitrogen (N), and phosphorus (P) is an ongoing global issue (Akinnawo 2023; Conley et al. 2009; Dillon and Molot 2024; Smith 2003; Smith and Schindler 2009). Run-off from excessive fertilization and the historical discharge of insufficiently treated wastewater has led to significant accumulation of P in aquatic environments, the so-called legacy sedimentary P (Dillon and Molot 2024; Tu et al. 2023). The seasonal release of this legacy P, that is,

internal loading, often sustains eutrophication, especially in shallow lakes (Kiani et al. 2020; Søndergaard et al. 1999; Søndergaard et al. 2007; Welch and Cooke 2005; Yin et al. 2022), leading to phytoplankton dominance, turbidity, and anoxic conditions (Ansari et al. 2010; Lürling et al. 2017; Waajen et al. 2014). Concurrently, P remains a critical and non-substitutable nutrient in the agricultural sector where it is essential for plant growth, and thus, continues to be a key component of fertilizers globally (Smith et al. 2015). However, the accessibility of the primary resource phosphate rock is limited to only a few countries worldwide, which has led to geopolitical conflicts and turned P into a limited, critical resource vulnerable to price fluctuations (Cordell et al. 2009; Crespi et al. 2022; Ibendahl 2022).

Consequently, the reuse of eutrophic sediments in agriculture (Braga et al. 2019; Canfield et al. 2024; Kiani et al. 2023) or the recovery of sedimentary legacy P from aquatic systems (Cakmak et al. 2022) is recently gaining more attention to expand circular economy principles on freshwater remediation and thereby foster more sustainable lake restoration (Tammeorg et al. 2024). The definite P removal from a eutrophic system can ensure long-term restoration of ecosystem balance (Kiani et al. 2020) while P recycling from the presumptive waste product, that is, dredged sediment, follows the principles of circular economy (Haasler et al. 2024; Kiani et al. 2021).

Eutrophication mitigation, that is, lake restoration, often aims at internal nutrient immobilization, such as capping via metal salts (Copetti et al. 2016; Huser et al. 2016) or oxygenation. If Fe salts or artificial oxygenation in a naturally Fe-rich system are applied (Boers et al. 1992; Copetti et al. 2016; Hupfer et al. 2016; Kleeberg et al. 2013), it consequently leads to an increase of redox-sensitive Fe(III)-bound P (Fe(III)-P), which is often described as a temporary P sink but also a source for internal P loading (Kiani et al. 2020; Reitzel 2005; Sondergaard et al. 2001; Yuan et al. 2020). Meanwhile, there is increasing recognition that the more stable redox-insensitive Fe(II)-bound P (Fe(II)-P) can play a significant role in the long-term burial or as a potential recovery phase of P in freshwater sediments (Heinrich et al. 2022; O'Connell et al. 2015; Reitzel et al. 2005; Rothe et al. 2014; Vuillemin et al. 2020).

Vivianite [$Fe_3(PO_4)_2{\cdot}8H_2O$] is often described as one of the most stable naturally occurring Fe(II)-P minerals in marine and freshwater sediments, as well as waterlogged terrestrial environments (Lenstra et al. 2018; Nriagu 1972; Rothe et al. 2016). Vivianite formation is favored in a reduced environment, at neutral pH, and under high Fe^{2+} and P but low free sulfide availability (Liu et al. 2018; Nriagu 1972; Rothe et al. 2015; Zhang et al. 2022). In the environment, vivianite is often defined as a group of minerals including its pure form, Mn, Mg, or Ca Fe-substituted phases, and various oxidation products as it rapidly oxidizes upon oxygen exposure (Kubeneck et al. 2023; Nriagu and Dell 1974; Nriagu 1972; Rothe 2016). Such oxidation products can be metavivianite [$Fe^{2+}Fe^{3+}{}_2(PO_4)(OH)_2{\cdot}6H_2O$] (Rothe et al. 2014) or santabarbaraite [$Fe^{3+}{}_3(PO_4)_2(OH)_3{\cdot}5H_2O$] (Fagel et al. 2005), which were formerly summarized as a group of hydrated Fe(II, III) orthophosphates named kertschenite (Nriagu 1972). Paramagnetic properties of vivianite have led to the development of magnetic extraction technologies from sewage sludge (Prot et al. 2019; Wijdeveld et al. 2022). Based on such technologies, mineral mining from freshwater sediments—particularly the magnetic extraction of vivianite from dredged sediment and reuse as, for example, fertilizer—could potentially promote more sustainable lake restoration and a circular economy as mentioned above. Hence, induced vivianite formation could facilitate long-term P burial and potentially recovery simultaneously.

In fact, the Fe speciation or Fe(III)/Fe(II) distribution in lake sediments can vary significantly depending on abiotic and biotic environmental factors, such as changing redox conditions, pH, or microbial activity, and variations in catchment or background geology (Beckler et al. 2015; Evans et al. 2004; Parsons et al. 2017). Additionally, sulfur (S) controls the availability and reactivity of Fe in aquatic systems (Heinrich et al. 2022; Kleeberg 1997; Rothe et al. 2015). Consequently, the sedimentary Fe-P speciation can be highly heterogeneous, with differences in P-binding strength among the phases and, therefore, P bioavailability for crop (Haasler et al. 2024). Well-known ferric specimens are amorphous or poorly crystalline ferric Fe(oxy)hydroxides, for example, goethite, ferrihydrite, hematite (Weng et al. 2012) which can adsorb or surface-complex P. In freshwater sediments, the most common ferrous minerals in which P is incorporated in the mineral lattice are vivianite and its various transformation and oxidation products (Nriagu and Dell 1974; Rothe 2016). However, various non-P bearing Fe(II) minerals, such as siderite [$FeCO_3$], or ankerite [$Ca(Fe^{2+},Mg)(CO_3)_2$], as well as mixed-valent Fe-oxides exist, such as magnetite [$Fe^{2+}Fe^{3+}{}_2O_4$] or green rust [$Fe^{2+}{}_4Fe^{3+}{}_2(OH^-)_{12}$] (Nriagu and Dell 1974).

Hence, detailed and reliable knowledge about the Fe-bound P species distribution is crucial (1) to understand internal P dynamics in lakes, (2) to evaluate the success or failure of eutrophication mitigation approaches aiming at nutrient immobilization, and (3) to develop P recovery strategies. In particular, vivianite quantification remains rather difficult and often relies on expensive and hardly accessible technologies, such as Moessbauer spectroscopy or synchrotron-based x-ray technologies including XAS or x-ray diffraction (XRD). Sequential P extraction (SPE) is a well-known and established method for quantifying operationally defined P pools in freshwater sediments with several protocols available (Paludan and Jensen 1995; Reitzel 2005; Wang et al. 2013). Moreover, SPE is a cheaper and more easily accessible alternative to other direct detection or characterization methods. However, most of the common SPE protocols do not distinguish between Fe(III)- and Fe(II)-P, even though the high importance of both phases is well-known and multiple Fe extraction protocols exist to

determine Fe(III) and Fe(II) separately (Heron et al. 1994; Phillips and Lovley 1987; Wallmann et al. 1993).

The chemical quantification of Fe(II)-P, primarily vivianite, as a separate phase from Fe(III)-P was originally proposed by Li et al. (2012) and optimized by Gu et al. (2016) using the Fe(II) complexation agent 2,2′-bipyridine (Bipy). Bipyridine is an organic compound and strong Fe(II) chelator (Smith et al. 2021). The release of vivianite-P by Bipy is facilitated through the complexation of aqueous Fe(II) (Eq. 1) thereby shifting the equilibrium equation toward vivianite dissolution (Eq. 2):

$$Fe^{2+}{}_{(aq)} + 3\,Bipy_{(aq)} \rightarrow [Fe(Bipy)_3]^{2+}{}_{(aq)} \quad (1)$$

$$Fe_3(PO_4)_2 \cdot 8H_2O_{(solid)} \leftrightarrow 3Fe^{2+}{}_{(aq)} + 2PO_4{}^{3-}{}_{(aq)} + 8H_2O \quad (2)$$

In Gu et al. (2016), the selectivity for vivianite-P and effectivity of the Bipy extraction step was tested and optimized by extracting a range of Fe mineral references and homogenized surface sediment samples (upper 10 cm) from one lake (< 4 m deep). Finally, the Bipy extraction step was inserted in the SEDEX protocol designed for marine sediment based on (Ruttenberg 1992). More recently, a SPE protocol incorporating the Bipy extraction step into a freshwater sediment protocol based on Reitzel (2005) was established and validated; however, for use with sewage sludge (Wang et al. 2021). In both studies, the 0.2% Bipy in 0.1 M KCl extractant was found to be selective for Fe(II)-P assigned to vivianite and to deliver robust results when inserted in the SPE protocols without the use of a glovebox.

The aim of the present study was to test whether the Bipy extraction step is a suitable tool for identifying and quantifying vivianite in a range of freshwater sediments with different compositions. Therefore, seven freshwater sediments from three European countries (Denmark, Germany, The Netherlands) with varying total sedimentary Fe and P content as well as restoration histories (Table 1) were extracted using the Bipy modified SPE by Wang et al. (2021) and the conventional SPE protocol based on Reitzel (2005) in parallel. For vivianite detection and to further support the extraction results, a range of direct, primarily qualitative, mineral detection methods was applied. These included the spectroscopic methods x-ray absorption near edge structure (XANES) at the Fe and P K-edge, XRD, as well as optical microscopy (Opt-Mic) and scanning electron microscopy with energy dispersive x-ray spectroscopy (SEM–EDX).

Materials and procedures

Study lakes

The seven study lakes were selected based on differences in sedimentary Fe and P contents, resulting in a range of Fe : P molar ratios, as well as varying restoration histories. A summary of the lakes' characteristics and histories is shown in Table 1 and as supplementary material (Section A).

Sediment sampling and characterization

Sediment was obtained as intact cores ($n = 3$ for Lake Ørn and Lyng; the rest $n = 1$) using a gravity core sampler and Kayak tubes from the deepest part of each lake. The intact sediment cores were either stored at 4°C until further use (Lakes Ørn, Lyng, Almind, and De Kuil) or sectioned directly in the field (Lakes Ouderkerkerplas, Groß Glienicker, Arendsee). Sampling dates, sectioning patterns, and respective motivations can be found as supplementary material (Section B). The samples were processed quickly and stored in airtight, dark conditions to minimize oxygen exposure. Airtight storage conditions were achieved by filling the storage vials completely with the fresh sediment and leaving no airspace. In the case of plastic zipper bags, the air was removed from the bag before closing. The dry matter content (DM%) was determined by weight loss after ~ 24 h at 105°C, followed by the determination of organic matter content as loss of weight after ignition (LOI%) at 520°C (450°C for Arendsee and Groβ Glienicker) for 5 h. The elemental composition of the sediment was determined after hot acid digestion (8 mL 1 M HCl, 1 h, 120°C) of ~ 0.1 g combusted sediment (520°C, 5 h). Contents of Fe, P, Al, Ca, Mg, and Mn were analyzed in the digestates using inductively coupled plasma optical emission spectroscopy (ICP-OES; Optima 2100 DV, Perkin Elmer). Sediment depth profiles of determined elemental compositions, molar Fe : P ratios, and LOI% can be found as supplementary material (Figs. S1 and S2).

Sequential P extraction

The fresh, sectioned sediment samples were subjected to both the conventional (Con) protocol by Reitzel (2005) and modified (Mod) protocol by Wang et al. (2021) in parallel. An overview of the extraction conditions and the corresponding P fractions can be found in Table 2 and as SI (Section C). For a detailed description of both SPE protocols, refer to Paludan and Jensen (1995), Reitzel (2005), and Wang et al. (2021). Briefly, 25 mL of extractant solution of varying strength and specificity were sequentially added to ~ 1 g fresh sediment in 50 mL centrifuge tubes (solid : liquid ratio 1 : 25), shaken horizontally on a table shaker (100 rpm, 1–24 h), and centrifuged (3000 rcf, 10 min) for solid–liquid separation. After each extraction step, the sediment residue was washed (shaking for 10 min, 100 rpm) at least once with the extractant solution and at least once with Milli-Q water. The supernatants from the extraction and washing steps were collected and combined per extractant for analysis, while the pellet remained in the centrifuge tube for the next extraction step. Soluble reactive phosphorus (SRP) (or inorganic P, hereafter iP) was measured spectrophotometrically using the standard molybdenum blue method (Murphy and Riley 1962). Total dissolved P (TP) in all fractions, and total dissolved Fe in the Bipy and BD fractions were determined via ICP-OES. The difference between TP and iP in the extractions was referred to as non-reactive P (NRP), which was interpreted as released labile organic P. Sum NRP represents the sum of NRP in the H_2O, Bipy, BD, and NaOH fractions, except for

Table 1. Lake characteristics (name, location, depth, surface area), history, and data on vivianite occurrence and detection if available in the seven lakes. For sedimentary molar Fe : P ratios please refer to SI, Fig. S2.

Lake characteristics	History	Vivianite occurrence	Reference(s)
Ørn Silkeborg, Denmark (56.154818, 9.519001) Mean depth 4 m; max. depth 10.5 m; 0.42 km^2	Catchment area mainly old forest (peat), very Fe-rich sediment, stratifying	Authigenic vivianite formation with homogenous depth distribution	O'Connell et al. (2015)
Lyng Silkeborg, Denmark (56.158597, 9.543975) Mean depth 2.4 m; max. depth 7.6 m; 0.1 km^2	Eutrophic, stratifying, received untreated sewage from Silkeborg until the 50s, nitrate [$Ca(NO_3)_2$] treatment in 1995 (dissolved), and 1996 (granulated)	No data	Søndergaard et al. (2000)
Almind Silkeborg, Denmark (56.148635, 9.543953) Max. depth 20.5 m; 0.52 km^2	Oligotrophic, stratifying	No data	Jørgensen et al. (2011) Robertson and Thamdrup (2017)
Groß Glienicker Berlin, Germany (52.465807, 13.110804) Mean depth: 6.8 m; max. depth: 11 m; 0.67 km^2	Formerly highly eutrophic, now mesotrophic; combined 50% $FeCl_3$ (dissolved) and 50% $Fe(OH)_3$ (solid) treatment 1992/1993 (500 g Fe m^{-2}), aeration	On average 20% of TP in upper 20 cm of sediment; increasing crystallinity with depth	Wolter (2010) Rothe et al. (2014) Heinrich et al. (2022)
Arendsee Altmark, Germany (52.890374, 11.475896) Mean depth: 29 m; max. depth 49 m; 5.14 km^2	Highly eutrophic; stratifying, hard water lake, groundwater-fed; hypolimnetic withdrawal, calcareous littoral mud was spread in profundal zone for P trapping (1995)	Present in sediment layers > 26 cm (Mn-rich), richest layers 30–36 cm	Findlay et al. (1998) Rothe et al. (2015) Hupfer et al. (2016)
De Kuil Breda, Netherlands (51.622351, 4.706393) Max. depth 9 m; 0.067 km^2	Eutrophic, shallow, stratifying, sand mining lake from the 50s, one-third filled with desalinated sea sand (2000), Flock ($FeCl_3$), and Lock (Phoslock®) treatment (May 2009)	No data	Waajen et al. (2016)
Ouderkerkerplas Amsterdam, Netherlands (52.290723, 4.930541) Max. depth 43 m; 0.073 km^2	Sand mining lake, cooling water discharge from hypolimnion since 2011, installed continuous bottom oxygenation system; peat and clay	No data	Stroom et al. (2010)

Lakes Arendsee and Groβ Glienicker, where NRP was only determined in the NaOH fraction (NaOH-NRP). The sum of extracted P pools (Sum_{ex}) was calculated as follows (Eq. 3):

$$Sum_{ex} = \sum TP\ content\ of\ all\ extracted\ fractions \quad (3)$$

Changes in the P fractions in response to the Bipy-step insertion were analyzed by normalizing the content of the fractions with Sum_{ex} and subsequently calculating the difference between the results of Mod and Con (ΔFraction in % of Sum_{ex}; Eq. 4):

$$\Delta\text{Fraction}(\%\text{of}\ Sum_{ex}) = \left[\frac{Fraction\ Mod\,(\mu mol\,P\,g^{-1}\,DW)}{Sum_{ex}\ Mod\,(\mu mol\,P\,g^{-1}\,DW)} - \frac{Fraction\ Con\,(\mu mol\,P\,g^{-1}\,DW)}{Sum_{ex}\ Con\,(\mu mol\,P\,g^{-1}\,DW)}\right] \times 100 \quad (4)$$

Hence, a negative value indicates loss, while a positive value indicates gain of the respective fraction. The H_2O fraction was excluded from ΔFraction analyses, as it was assumed to be unaffected due to its extraction prior to the Bipy step.

Note that due to discrepancies in protocol routines, the extracts from Lakes Groβ Glienicker and Arendsee were filtered (0.45 μm syringe filter) and digested using wet oxidation (5% $K_2O_8S_2$) before P measurements. Hence, these values represent dissolved total P (DTP) but are labeled as iP for simplification. It should be noted, however, that wet oxidation hydrolyzes dissolved organic P (NRP) to iP, which may slightly overestimate iP in the extracts from these two lakes. Further, Humic-P was determined in all lake sediments except Arendsee and Groβ Glienicker, and Residual-P only in Lakes Almind, Lyng, and Ørn.

Direct detection methods

To validate the extraction results, confirm the presence or absence of vivianite-P, and better distinguish between

Table 2. Summary and description of the extraction steps used in this study, including the Bipy step inserted between H_2O and BD highlighted by dashed lines. RT denotes room temperature. A full schematic of the protocol can be found as SI (Fig. S3).

Extractant solution	Extraction conditions	Washing step	Assigned P fraction
N_2-purged milli-Q	1 h, RT	1× milli-Q	H_2O-iP Porewater/exchangeable
0.2%-2,2′-bipyridine +0.1 M KCl	24 h, 50°C	1× 0.2% Bipy in 0.1 M KCl, 2× 0.1 M KCl, 1× milli-Q	Bipy-iP Fe(II)-bound / vivianite
0.11 M bicarbonate-dithionite (BD)	1 h, RT	2× 0.11 M BD, 1× milli-Q	BD-iP Redox-sensitive Fe/Mn bound
0.1 M NaOH	16 h, RT	1× 0.1 M NaOH, 1× milli-Q	NaOH-iP Metal Fe/Al bound
1 M HCl	Filtration of NaOH, digestion of filter 1 h, 120°C	None	Humic-P Humic acids bound
0.5 M HCl	1 h, RT	1× milli-Q	HCl-P Ca-bound
1 M HCl	Digestion (1 h, 120°C) of 520°C—5 h ignited pellet	None	Residual-P Refractory

amorphous and crystalline phases, one sediment depth with the highest Bipy-iP content determined using SPE was selected for each lake and further characterized using XANES at the Fe and P K-edge and XRD (Fig. 1). Hereafter, these selected sediment samples are referred to as follows: DK (De Kuil 0–1 cm), OKKP (Ouderkerkerplas 0–1 cm), AL (Almind 12–13 cm), AS (Arendsee 36–37 cm), GG (Groß Glienicker 0–1 cm), ØN (Ørn 19–20 cm), and LY (Lyng 0–1 cm). An additional sample from Lake Ørn sediment (0–2 cm pooled) was analyzed using Fe XANES before (Ørn B) and after (Ørn A) the Bipy extraction. Lake Ørn is known to contain a significant amount of vivianite from an earlier study (O'Connell et al. 2015). The samples AL, AS, GG, ØN, and LY were also visualized using Opt-Mic and SEM–EDX. Note that, due to a lack of material, XRD analysis for Lake De Kuil was conducted on a deeper sediment layer where the second highest Bipy-iP concentration was detected (14–15 cm). To prepare sediment for the various analytical methods, fresh sediment was placed at −20°C overnight and subsequently freeze-dried (2–3 d, 0.2 mbar, −50°C). Freeze-drying is common practice to preserve samples for, for example, XAS analysis (Herzog et al. 2024; Karlsson et al. 2008). The freeze-dried sediment was then stored in dry, airtight, and dark conditions until further analysis.

X-ray absorption near edge structure at the Fe and P K edge

To identify the overall Fe speciation before and after Bipy extraction and in the selected sediment samples, XANES spectra at the Fe Kα1-edge were obtained at the Canadian Light Source (CLS) in Saskatoon, Saskatchewan, Canada, using the Soft X-ray Micro Characterization Beamline (SXRMB). Reference materials and samples were thinly spread on double adhesive carbon tape attached to a Cu sample holder. Each spectrum was collected in both total electron and fluorescence yield modes in at least duplicates. The detector distance was set to 100 mm. The step size was 2 eV in the pre-edge region (7076–7106 eV), 0.35 eV at the edge step (7106–7152 eV), and 0.75 eV in the post-edge region (7152–7262 eV). Dwell time was set to 1 s for all three regions.

To identify the overall P speciation, bulk XANES spectra at the P Kα1-edge were obtained at the Synchrotron Light Research Institute (SLRI) in Nakhon Ratchasima, Thailand, at the X-ray Absorption Spectroscopy Beamline end station BL8 (DK, OKKP, AL), and the CLS in Canada (AS, GG, ØN, LY). At the SLRI, all references and samples were diluted to 0.2 wt% (2 g P kg^{-1} DW) with silicon dioxide (SiO_2, form: sand, CAS: 60676-86-0, Sigma-Aldrich), following Prietzel et al. (2016), and homogenized using a ZrO_2 ball mill (Fritsch, pulverisette 23, 30 s^{-1} frequency, 5–10 min). Reference materials and samples were thinly spread on a metal frame sterilized with ethanol and sealed on one side with sticky Nitto tape. All spectra scans were collected in fluorescence mode in an He gas environment in duplicates. The detector distance was set to 220 mm. The step size was 5 eV in the pre-edge region (2145.5–2132.5 eV), 0.2 eV at the edge step (2132.5–2195.5 eV), and 5 eV in the post-edge region (2195.5–2295.5 eV), with a dwell time of 3, 6, and 3 s, respectively. At the CLS, sample preparation, handling, and measurement of P XANES were the same as described for Fe XANES, except that the detector distance was set to 40 mm for reference and 5 mm for samples. The step size was 1 eV in the pre-edge region (2112.5–2139.5 eV), 0.15 eV at the edge step (2139.5–2170.5 eV), and 0.75 eV in the post-edge region (2170.5–2210.5 eV), with a dwell time of 1 s each.

The Fe and P XANES spectra were energy calibrated by setting the first inflection point of Fe(0) to 7111.08 eV (Wilke

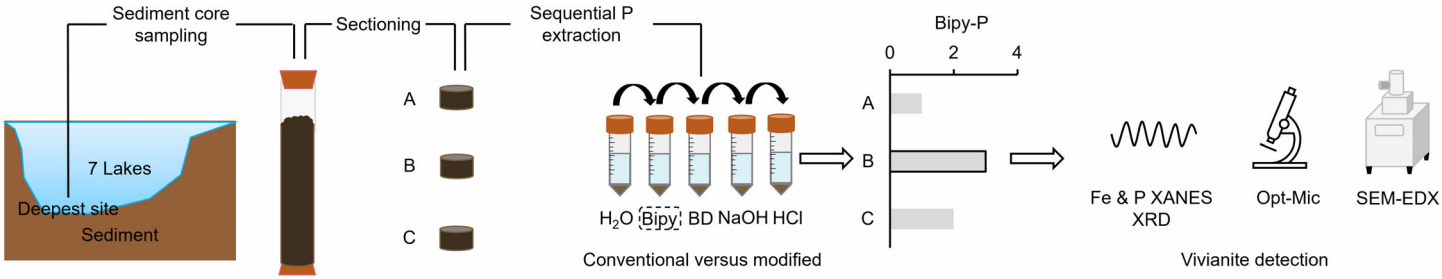

Fig. 1. Schematic of experimental set up and workflow.

et al. 2001) and to 2145.5 eV for elemental P powder (Prietzel et al. 2016). The spectra were averaged using the Sixpack software (Webb 2005). Subsequently, spectra were background-corrected using a linear regression fit through the pre-edge region and normalized to a one-unit edge jump of the total K-edge intensity. A linear combination fitting (LCF) analysis was employed to estimate the proportions of various Fe or P phases in the samples. Linear combination fitting was performed at −10 to +30 eV around the absorption edge using SixPack, allowing the E_0 to float and applying non-negative boundary conditions. The sum of the weights of the standards used was not forced to equal 1. Components with a contribution of <5 wt% were excluded from the results. Chi-squared values were used to assess the goodness-of-fit.

To qualitatively compare the XANES region from the before and after scan of Lake Ørn B and A, SixPack (Webb 2005) and FityK (Wojdyr 2010) were used. Pre-edge centroid energy was determined according to the method outlined by Wilke et al. (2001). In summary, the energy-calibrated spectra were baseline-corrected and normalized. To extract the centroid position, a spline baseline was manually adjusted around the pre-edge region, following Wilke et al. (2001). The baseline-corrected pre-edge was then fitted using two pseudo-Voigt functions (comprising 50% Gaussian and 50% Lorentzian components), and the centroid was calculated based on the resulting peak areas and positions.

For the LCF fitting of Fe, the following reference materials were used: ankerite [$Ca_2MgFe(CO_3)_4$], crystalline Fe(III)-P [$Fe^{3+}PO_4 \bullet 2H_2O$] (strengite; Sigma-Aldrich, CAS No.: 13463-10-0), amorphous Fe(III)-P [$Fe^{3+}PO_4$] (in vitro synthesized; SI Section D, Fig. S4), Fe complexed to Suwannee Rives fulvic acid (OM-Fe), ferrihydrite [$(Fe^{3+})2O_3{\cdot}0.5H_2O$] (Karlsson and Persson 2012), FeS, pyrite [FeS_2], lazulite [$(Mg,Fe^{2+})Al_2(PO_4)_2(OH)_2$], and vivianite [$Fe^{2+}{}_3(PO_4) \bullet 8H_2O$] (in vitro synthesized; SI Section D).

The reference material used for P included monazite [$(Ce,La,Y,Th)PO_4$], crystalline and amorphous Fe(III)-P as described for Fe XANES (spectral contributions of the crystalline and amorphous Fe(III)-P were combined as Fe(III)P), the synthetic vivianite (vivianite-P), hydroxyapatite [$Ca_{10}(PO_4)_6(OH)_2$] (HAp; Macron™ Chemicals, CAS No.: 1306-06-5), tricalcium phosphate [$Ca_3O_8P_2$] (CaOP; Sigma-Aldrich, CAS No.: 7758-87-4), $AlPO_4$ (AlP; RDH Laborchemikalien GmbH & Co KG, CAS No.: 7784-30-7), and phytic acid bound P [$C_6H_{18}O_{24}P_6$] (Sigma-Aldrich; CAS No.: 83-86-3).

X-ray diffraction

To identify crystalline mineral phases, powder XRD diffractograms were collected using Cu Kα radiation at 40 kV and 15 mA with a step size of 0.02 and a scanning rate of 10°/min in a 2θ range from 5° to 70° (Rigaku Miniflex 600, Japan). Before loading into the sample holder, samples were homogenized using an agate mortar and pestle. Sample holders were sterilized with ethanol before filling.

Optical microscopy and scanning electron microscopy with energy dispersive x-ray spectroscopy

Vivianite turns blue upon surface oxidation (Nriagu 1972). For visualization and preparation for SEM–EDX analysis, a few sediment particles were placed on a sample holder with carbon tape to secure them in place. These were screened for blue-colored particles using the light microscope Leica MZ95 equipped with a Leica DFC320 camera. Once the area of interest was located, the sample holder was placed in a vacuum chamber and coated with a 10 nm layer of gold using a JEOL JFC-1200 fine coater to make the sample surface electrically conductive. Subsequently, SEM–EDX analysis was conducted using a JEOL JSM-6480 LV scanning electron microscope (SEM) equipped with an Oxford Instruments x-act SDD energy-dispersive x-ray (EDX) spectrometer. The accelerating voltage was set to 15.00 kV, and the working distance was 10 mm. The software JEOL SEM Control User Interface for the SEM and Oxford Instruments Aztec for the EDX data processing were used.

Assessment

Fe x-ray absorption near edge structure before and after the bipyridine extraction

The pre-edge analysis of the Fe XANES spectra following the procedure of Wilke et al. (2001) indicated that the surface sediment from Lake Ørn (0–2 cm) contained both Fe(II) and Fe(III). A more accurate determination of the Fe(II) : (III) ratio

was hindered by the uncertainty surrounding the coordination chemistry in these samples. However, the Bipy extraction resulted in a shift of the centroid position from 7112.5 to 7112.7 eV, indicating predominant removal of Fe(II) containing Fe minerals (Fig. 2). The LCF analysis revealed that primarily vivianite but also a partially Fe-OM was removed from the matrix by the Bipy extraction (Table 3).

Comparison of extraction results

The overall extraction results from the Con and Mod SPE protocols are presented in comparison for each lake in Fig. 3. The sum of extracted P pools (Sum_{ex}) did not differ significantly between the two protocols, which was evaluated by using linear regression analysis on the correlation between the Sum_{ex} obtained from Con and Mod ($R^2 = 0.99$, $p < 0.001$; Fig. S5). The differences between Sum_{ex} using Con and Mod ranged from 0.06 to 36% of sedimentary TP, of which 10 out of 57 data points were > 10%. Hence, there was no substantial loss of extraction efficiency after the insertion of the Bipy step.

According to the results of the Mod protocol, the BD fraction, representing redox-sensitive Fe(III)/Mn(IV) bound P, was the most important fraction in Lakes Ørn, Lyng, Almind, Groβ Glienicker, and Arendsee (21–83% of Sum_{ex}). Contrastingly, in Lakes Ouderkerkerplas and De Kuil, the HCl fraction (Ca-bound P) was predominant throughout depth (11–91% of Sum_{ex}). Further, the NaOH fraction, representing metal (Fe/Al) bound P, played an important role in Lakes Ørn, Lyng, and Groβ Glienicker (3–26% of Sum_{ex}), but less in Lakes Almind, Ouderkerkerplas, De Kuil, and Arendsee (< 2–10% of Sum_{ex}). The labile organic P fractions, Humic-P and Sum NRP, accounted for 1–21% and 0.8–27% of Sum_{ex}, respectively. The H_2O fraction and Residual-P were of minor importance for the sedimentary P speciation (both on average 2% of Sum_{ex}).

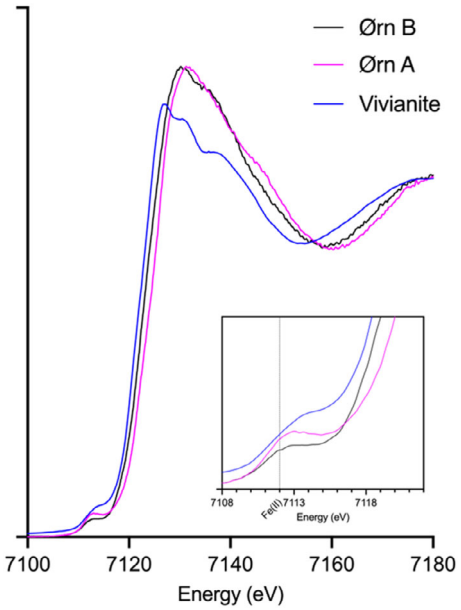

Fig. 2. Fe K-edge XANES scans of Lake Ørn sediment (0–2 cm) before (Ørn B; black) and after (Ørn A; pink) the Bipy extraction, and the vivianite reference (blue). The insert shows a close up of the pre-edge region, and the dashed line at 7112 eV indicates Fe(II).

Among all lakes, most Bipy-iP was extracted in Lake Ørn (19–33% of Sum_{ex}) and Lyng (28–43% of Sum_{ex}), with a homogeneous depth distribution, peaking at 19.5 cm and 0.5 cm sediment depth, respectively. Lakes Arendsee and Groβ Glienicker contained moderate Bipy-iP concentrations (9–29% and 20–38% of Sum_{ex}, respectively). In Lake Arendsee, Bipy-iP showed a sharp increase with depth, peaking at 36.5 cm sediment depth, whereas in Lake Groβ Glienicker, Bipy-iP peaked near the surface at 0.5 cm and decreased with depth. The lowest Bipy-iP concentrations were found in Lakes De Kuil < Ouderkerkerplas < Almind (0–4%, 0–18%, and 13–33% of Sum_{ex}, respectively), with peaks at 0.5, 0.5, and 12.5 cm sediment depth, respectively.

Changes in the different P fractions

The extent of ΔFraction generally matched well with the determined Bipy contents with few exceptions (Figs. 4 and S6). Thus, the loss of a pool when using Mod primarily indicated a shift into the Bipy extract. In ØN, the NaOH pool mainly contributed to the Bipy extract, while in OKKP, AS, and LY it was primarily the BD pool. In AL and GG, a combination of contributions from the BD and NaOH pools was detected. Overall, the observed changes in Humic- and Residual-P were marginal and negligible. However, Sum NRP slightly increased in 4 out of 5 samples, and NaOH-NRP decreased in GG and AS, indicating a minor shift of labile organic P (Fig. S10). These observations are in line with the predominant removal of Fe(II) minerals, primarily vivianite, and the partial reduction of Fe-OM in lake Ørn (0–2 cm) as recorded with Fe XANES (Fig. 2; Table 3).

While the BD fraction is generally interpreted as redox-sensitive Fe(III)/Mn(IV) bound P, NaOH quantifies more strongly bound metal phases, such as Fe- and Al-bound P (Gu et al. 2020; Paludan and Jensen 1995; Reitzel 2005).

Table 3. LCF analysis of the Fe XANES spectra collected from Lake Ørn sediment (0–2 cm) before (Ørn B) and after (Ørn A) Bipy extraction. Results presented as spectral contributions (wt%).

Spectral contribution (wt%)	Ørn B	Ørn A
Vivianite	29	–
Fe-OM	39	16
Crystalline Fe(III)P	5	33
Ferrihydrite	28	36
Goethite	–	10
Pyrite	–	5
Chi-squared	0.16	0.04

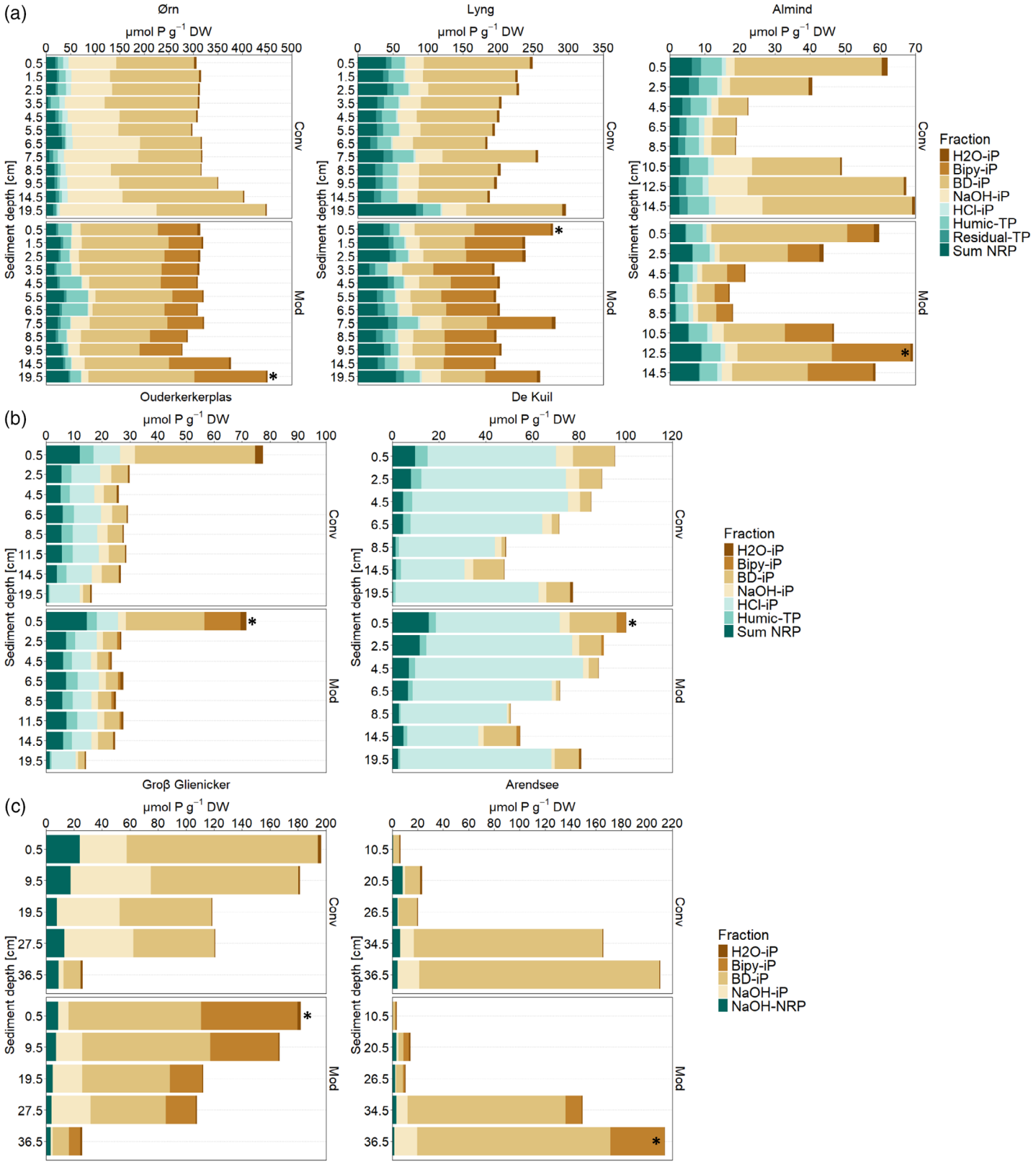

Fig. 3. SPE extraction results from the conventional (Con) and modified (Mod) protocol: Lakes (**a**) Ørn, Lyng, Almind, (**b**) Ouderkerkerplas, De Kuil, and (**c**) Groβ Glienicker and Arendsee. Note the differences in x- and y-scales, and legend. Asterisks indicate the sediment depth chosen for characterization with direct detection methods.

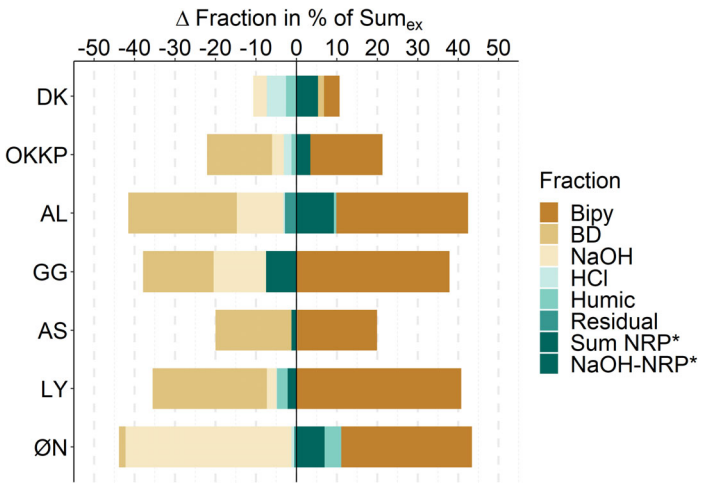

Fig. 4. Change of the individual P fractions (ΔFraction) in % of Sum_{ex} after application of the modified sequential P extraction protocol including the Bipy extraction. Only one sample per study lake is presented at the sediment depth with the highest Bipy-iP content detected. Negative values represent loss, positive gain of the respective fraction. *Note: Sum NRP and NaOH-NRP are the same color, since both fractions represent labile organic P. However, Sum NRP summarizes NRP in the H2O, Bipy, BD, and NaOH fraction except for AS and GG, for which only NaOH-NRP was determined.

However, due to a low sedimentary Al and Mn content compared to Fe (Fig. S1), it can be assumed that both the BD and NaOH fractions were primarily Fe-bound P. Vivianite can exist in various levels of crystallinity and oxidative states, often described as a group of oxidative products, that is, mixed Fe(II)/Fe(III)-P phases named kertschenite (Palache et al. 1952), or metavivianite and santabarbaraite (Fagel et al. 2005; Rothe et al. 2014) as described in the introduction. Bipy appeared to also capture these P species well, as it mobilized both P, P which would have been extracted by BD and NaOH using the conventional protocol.

Fe and P release by bipyridine

The Bipy-extractable total Fe and P contents and the resulting molar Fe : P ratio in the Bipy extract can be found in Tables 4 and 5. Only two out of seven lakes, Lake Almind and Lyng, showed a significant positive linear correlation between Fe and P release. Additionally, the reported molar Fe : P ratios in the Bipy extract ranged from 2.4 to 32.4, which deviate from the theoretical molar Fe : P ratio of 1.5 reported for pure vivianite (Al-Borno and Tomson 1994; Nriagu 1972).

This indicates that there are other Fe(II) sources than pure vivianite during the Bipy extraction, and that also non-P-bearing Fe(II) phases were extracted. Possible Fe(II)-P phases could be oxidation products of vivianite, such as hydrated Fe(II, III) orthophosphates summarized as kertschenite (Palache et al. 1952), as well as amorphous ferric phosphate and strengite [Fe^{2+}-$PO_4{\cdot}2H_2O$], or metavivianite [$Fe^{2+}Fe^{3+}{}_2(PO_4)(OH)_2{\cdot}6H_2O$] (ref) and santabarbaraite [$Fe^{3+}{}_3(PO_4)_2(OH)_3{\cdot}5H_2O$] (Fagel et al. 2005).

Table 4. Mean Bipy-extractable Fe and P contents ± SD as well as molar Fe : P ratios in the Bipy extract of selected sediment samples. NA = not available.

	μmol g^{-1} DW		Molar ratio
Sample (*n*)	Fe	P	Fe : P
DK (2)	124.9 ± 14.4	3.9 ± 0.03	32.4
OKKP (2)	39.4 ± 2.1	12.8 ± 0.95	3.1
AL (3)	270.4 ± 5.9	22.4 ± 0.77	12.1
AS (2)	100.5 ± 0.8	42.3 ± 0.96	2.4
GG (2)	174.8 ± 5.2	69.0 ± NA	2.5
ØN (1)	477.7 ± NA	145.9 ± NA	3.3
LY (1)	445.2 ± NA	126.7 ± NA	4.1

Table 5. Linear regression analysis of the Fe and P release in the Bipy extracts from all extracted sediment depths per lake.

	R^2 (*p* value)
Lake (*n*)	P vs. Fe
De Kuil (7)	0.47 (0.089)
Ouderkerkerplas (8)	0.18 (0.303)
Almind (8)	0.92 (< 0.001)
Arendsee (5)	0.59 (0.129)
Groß Glienicker (5)	0.73 (0.065)
Ørn (12)	0.03 (0.568)
Lyng (12)	0.94 (< 0.001)

Other non-P-bearing Fe(II) specimens known to occur in sediments could be ankerite [$Ca(Fe^{2+},Mg)(CO_3)_2$], siderite [$Fe^{2+}CO_3$], magnetite [$Fe^{2+},Fe^{3+}{}_2O_4$], or humic-complexed Fe(II) (Catrouillet et al. 2014). In addition, impurities in the vivianite crystal lattice are very common in environmental samples, for instance, Mn^{2+} or Mg^{2+} (baricite [$(Mg^{2+},Fe^{2+})_3(PO_4)_2{\cdot}8H_2O$]) may substitute for Fe^{2+} to a minor extent. Fe-substitution with Mn or Mg can, in turn, influence the crystal structure and size, as well as the morphology of vivianite (Kubeneck et al. 2023) which might impair its direct detection. For further discussion of the non-linearity and disproportional Fe and P release by Bipy, *see* Non-linearity between Fe and P release in the Bipy extraction section later in this article.

Fe and P x-ray absorption near edge structure on selected sediment depths

The LCF analysis of the Fe XANES spectra (Figs. S7 and S8) revealed a high contribution of vivianite in AS (55 wt%) and GG (20 wt%), and a moderate contribution in LY (15 wt%) and ØN (11 wt%) to the overall Fe speciation (Fig. 5A). Overall, AS, GG, ØN, and LY showed relatively high heterogeneity in Fe speciation. The most dominant Fe phase was ferrihydrite in all four sediments, except for AS, where the spectral contribution of vivianite outweighed that of other phases.

Contrarily, DK, OKKP, and AL appeared less heterogeneous, with the most dominant contributions from amorphous Fe(III)-P, followed by FeS and Fe-OM, and no contribution of vivianite. Crystalline Fe(III)-P was detected in LY, ØN, AS, and GG, but not in DK, OKKP, and AL.

The LCF analysis of the P XANES spectra (Figs. S7 and S8) confirmed the presence of vivianite in AL (62 wt%), AS (61 wt %), OKKP (26 wt%), ØN (16 wt%), and GG (13 wt%) but not in DK (Fig. 5B). Note, LCF of P XANES data could not be performed for LY due to poor spectra quality. While AL, AS, GG, and ØN primarily consisted of vivianite-P and Fe(III)-P, DK and OKKP showed a more heterogeneous P speciation. The DK sample mainly consisted of HAp, Fe(III)-P, with minor contributions of CaOP and monazite. In OKKP, the main species were Fe(III)-P, vivianite-P, AlP, and HAp. A minor fraction of phytic acid P was detected in OKKP and AL. In AS and GG, some contribution of HAp was found.

The relative contributions of Bipy-iP and -Fe (% of total P and Fe) were compared to the LCF results of both Fe and P XANES for the importance of vivianite (Table 6). Generally, both showed similar trends for the importance of vivianite. However, some discrepancies were found. In AL, vivianite was not detected by Fe XANES, but high importance was found with P XANES and Bipy-iP, although the extraction result was

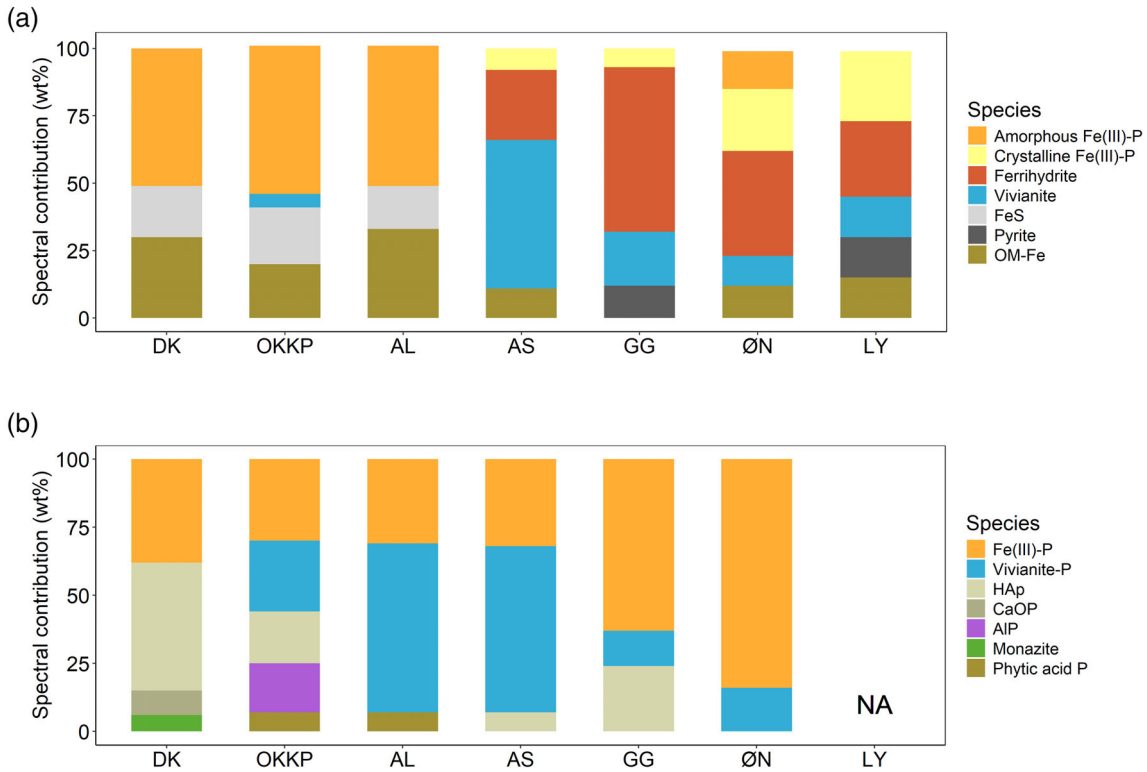

Fig. 5. Linear combination fitting (LCF) results in spectral contribution (wt%) of the Fe (**a**) and P (**b**) XANES spectra collected from the sediment layer with the highest Bipy-iP content (one sample per lake). Reduced X^2 for goodness of fit from left to right: (A) 0.27, 0.22, 0.44, 0.02, 0.03, 0.05, 0.01, and (B) 0.01, 0.01, 0.02, 0.04, 0.10, 0.02. NA = Not available.

Table 6. Fe and P extracted with Bipy in % of the total sedimentary Fe and P contents in comparison to LCF spectral contribution of vivianite determined with Fe and P XANES (wt%). NA = not available.

Sample	Bipy-Fe (% of TFe)	Fe XANES vivianite (wt%)	Bipy-P (% of TP)	P XANES vivianite (wt%)
DK	3	0	15	0
OKKP	7	5	17	26
AL	15	0	35	62
AS	16	55	16	61
GG	23	20	37	13
ØN	20	11	37	16
LY	58	15	43	NA

slightly lower than the spectral contribution. In AS, both Fe and P XANES reported a much higher share of vivianite compared to the Bipy extraction, indicating underestimation of vivianite using Bipy. On the contrary, in LY and ØN, Bipy-Fe reported a much higher importance than Fe XANES, and in ØN Bipy-iP was almost twofold the P XANES results. In GG, a similar trend was found for the P estimates (Bipy-iP threefold the XANES P estimate), while the Fe estimates matched well.

X-ray diffraction, optical microscopy, and scanning electron microscopy with energy dispersive x-ray spectroscopy

Important crystalline phases in the sediment samples were mostly quartz, Fe phosphates, calcite, bentonite, and zeolite (Table 7; SI Section H). X-ray diffraction signals for crystalline vivianite were detected only in AS (Table 7; SI Section H). Other crystalline Fe(II) phosphate minerals were detected only in AL (mixed valent Fe phosphate oxide, scorzalite). In LY, the predominance of pyrite reflections was noted.

According to the Opt-Mic and SEM–EDX analysis, blue-colored vivianite crystallites were observed in AS, GG, and ØN. The largest particle diameter was found in AS (150 μm)—which coincided with crystalline vivianite detection using XRD; followed by GG (100 μm), and finally ØN (50 μm) (Fig. 6; Table 7). Since Bipy-iP was present at notable levels in LY and AL (Figs. 3 and 5), these samples were also examined via Opt-Mic and SEM–EDX. However, no evidence of blue-colored vivianite particles was found (Fig. S9). The analyzed particles were $\sim$ 40 μm in diameter and contained Fe, Al, and P. In AL, it may be identified as scorzalite in combination with the XRD results, while in LY the phase of the particle remains unidentified.

Discussion

Vivianite detection and quantification with the bipyridine extraction

According to our Bipy extraction results, noteworthy vivianite-P contents were found in Lakes Lyng > Ørn > Groβ Glienicker > Arendsee (Fig. 2). Vivianite was confirmed to be present in these sediments by solid-state analysis with Fe and P XANES and SEM–EDX (Figs. 5 and 6); crystalline vivianite was only found in AS using XRD (Table 6). Vivianite was expected to be an important phase in these sediments since the underlying sedimentary elemental composition and restoration histories create favorable conditions for its formation (*see* Table 1). All four lakes are deep and stratifying and have either suffered from eutrophic conditions and high P loadings in the past or are currently experiencing them. Further, sedimentary Fe was high to excessive (Fig. S1). Both high P and Fe availability are important criteria for increased vivianite formation, as are a neutral to alkaline pH and a reducing, non-sulfidic environment (Liu et al. 2018; Nriagu 1972; Rosenqvist 1970; Rothe et al. 2015). Anoxic bottom water and thus reducing conditions are quite common in eutrophic or deep, stratifying lakes due to seasonal summer stratification, which results in a temporary anoxic water column above the sediment. This, in turn, can boost authigenic vivianite formation.

In Lake Ørn, significant authigenic vivianite formation during early diagenesis within the upper 10 cm of the sediment was reported by O'Connell et al. (2015). Below 10 cm, vivianite underwent crystallization processes during burial. In our study, Bipy-iP was homogenously high throughout the upper 20 cm, but slightly higher at 14.5 and 19.5 cm (Fig. 3). Further, O'Connell et al. (2015) estimated vivianite to account

Table 7. The main crystalline phases in selected sediment layers of the seven lakes detected via XRD, as well as qualitative analysis via SEM–EDX (particle diameter [μm], atomic weight % Fe : P ratio of the selected particle). The respective XRD diffractograms can be found as supplementary material (Section H).

		SEM–EDX		
Sample	XRD	Vivianite detected	Particle diameter (μm)	Fe : P (atomic weight%)
DK*	Quartz, gypsum, calcite, zeolite, bentonite	–	–	–
OKKP	Quartz, calcite, bentonite, iron hydrogen phosphate [$Fe_2(HPO_3)_3$]	–	–	–
AL	Quartz, mixed valent iron phosphate oxide [Fe(II),Fe(III) PO_5], scorzalite [$Fe^{2+}Al_2(PO_4)_2(OH)_2$]	No	–	–
AS	Calcite, vivianite, joosteite [$Mn^{2+}(Mn^{3+}, Fe^{3+})(PO_4)O$], quartz	Yes	150	3.0
GG	Quartz, bavenite [$Ca_4Be_2Al_2Si_9O_{26}(OH)_2$], piemontite [$Ca_4Be_2Al_2Si_9O_{26}(OH)_2$], calcite	Yes	100	3.1
ØN	Quartz, β-$FePO_4$	Yes	50	3.1
LY	Quartz, pyrite, muscovite [$KAl_2(OH,F)_2\|AlSi_3O_{10}$]	No	–	–

*XRD analysis performed at 14–15 cm sediment depth.

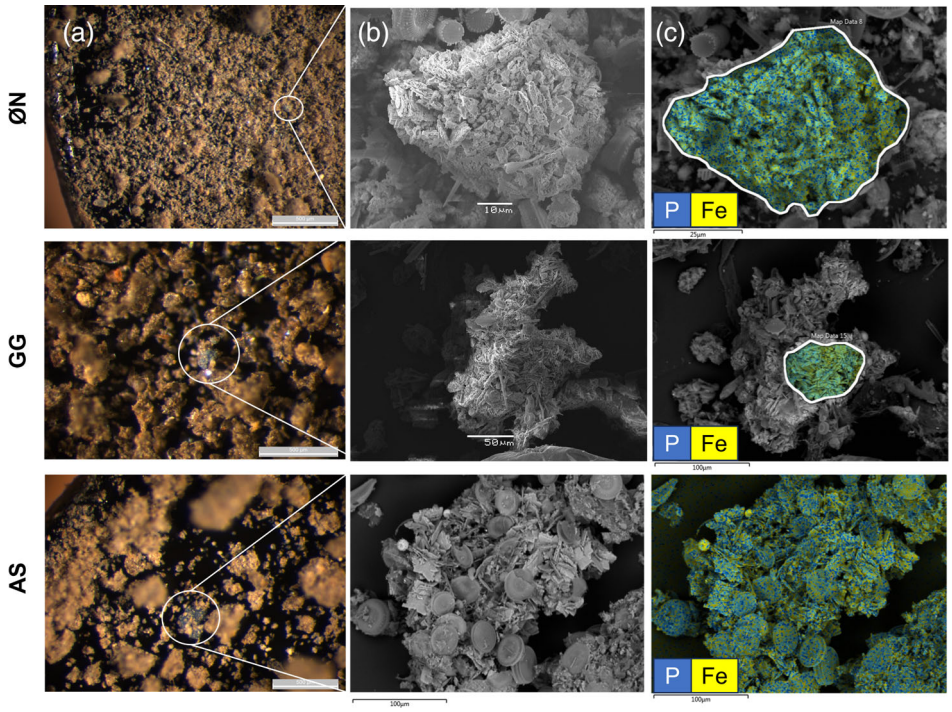

Fig. 6. Optical microscopy (**a**), SEM (**b**), and layered EDX images (**c**) from Lake Ørn (19.5 cm), Groβ Glienicker (0.5 cm), and Arendsee (36.5 cm) for Fe and P elemental mapping. The P signals are presented in blue and Fe signals in yellow. The areas with Fe and P overlapping appear thus in blue and are identified as vivianite. The atomic weight% Fe : P ratios were 3.1 in ØN, 3.1 in GG, and 3.0 in AS. For pure vivianite, the theoretical atomic weight% Fe : P ratio is 2.7.

for 3–5% of TFe and ∼ 26% of TP in the upper 10 cm. Likewise, in our study, Bipy-iP averaged ∼ 35% of TP in the upper 10 cm of the sediment, while Bipy-Fe accounted for ∼ 21% of TFe. The much higher Bipy-Fe can be attributed to the release of non-P-bearing Fe(II) species in the Fe-rich sediment, which explains the lack of correlation between the Fe and P release in the Bipy extract in Lake Ørn (Tables 4 and 5).

In Lake Groβ Glienicker, Bipy-iP was dominant in the upper 10 cm of sediment, decreasing with depth, and SEM–EDX analysis confirmed the presence of 100 μm sized vivianite crystallites at 0.5 cm sediment depth. Likewise, long-term P retention through ongoing authigenic vivianite formation and the presence of crystalline vivianite were reported by Rothe et al. (2014) and Heinrich et al. (2022) in this lake. Rothe et al. (2014) reported that ∼ 20% of TP was vivianite-P within the upper 20 cm of sediment, with low to absent vivianite-P contribution > 23 cm depth. According to our extraction results, vivianite-P was on average 26.6% of TP in the upper 20 cm, while still around 16% and 18% of TP was attributed to vivianite-P at 27.5 and 36.5 cm sediment depths, respectively. Quantitative XRD analysis in Heinrich et al. (2022) confirms the presence of crystalline vivianite in deeper sediment layers (9–11 and 19–21 cm) with increasing intensity of the vivianite signal with depth. Accordingly, a vivianite crystallite was detected in this sediment in our study by SEM–EDX analysis (Fig. 6).

Settlement and subsequent transformation during burial of amorphous Fe(III)-P is another prerequisite for vivianite formation in deeper, anoxic sediments (Heinrich et al. 2021; Scholtysik et al. 2022). In Lake Lyng, reduced hypolimnetic accumulation of Fe and P was observed in response to hypolimnetic nitrate dosing in the form of $Ca(NO_3)_2$ in 1995 and 1996. This suggests increased sedimentary P retention due to Fe(oxy)hydroxides-P precipitation (Søndergaard et al. 2000), followed by reductive dissolution and reprecipitation of vivianite-P in deeper, anoxic sediment layers. When using Fe XANES, the Fe speciation was revealed to be very heterogeneous in this sediment, while XRD analysis revealed no significant crystalline Fe-P phases. Moreover, Bipy extracted primarily BD-P (Fig. 3) and the Fe and P release in the Bipy extraction was significantly linearly correlated (Table 5). This indicates that the Fe-P binding forms in Lake Lyng sediment, including vivianite, are present as mixed valent, amorphous transformation and oxidation products as described before.

In Lake Arendsee, there was a sharp transition from non-vivianite-bearing sediment in the upper 20 cm to vivianite-rich sediment layers below. These depth profiles align with the observations made by Rothe et al. (2014) and Rothe et al. (2015), respectively. Also in Scholtysik et al. (2022) this sharp transition is described and was explained by changes in sulfide formation. Simultaneously, the Bipy extraction results revealed a similar depth profile. However, Bipy, predominantly

derived from the BD pool (Fig. 3), appeared to underestimate the vivianite content compared to the XANES LCF analysis (Table 6), while XRD and SEM–EDX analysis confirmed the presence of crystalline vivianite. This indicates that high crystallinity impaired the Bipy extraction efficiency and is discussed in more detail in the section Impact of level of crystallinity Bipy extraction efficiency.

Finally, Lakes Almind, Ouderkerkerplas, and De Kuil (in a descending order) were found to have low to absent sedimentary vivianite contents, that is, < 30 μmol g^{-1} DW (Fig. 2). All three lakes had very low total sedimentary P contents, ranging from <32 to 129 μmol g^{-1} DW (< 1 to 4 mg g^{-1} DW) and comparatively high molar Fe : P ratios (Figs. S1 and S2), which cannot result in significant vivianite contents. The relatively high importance of FeS and Fe-OM in these lakes, as detected via Fe XANES (Fig. 5A), suggests that P-Fe binding is outcompeted by S/OM-Fe binding, a phenomenon also suggested for other sulfide- or organic-rich freshwater systems (Heinrich et al. 2022; Kleeberg et al. 2013; Rothe et al. 2015).

Furthermore, the lakes' restoration histories (Table 1) alongside Fe(II)-consuming or -scavenging processes in the sediment can reduce the Fe(II) availability for vivianite formation. For example, the addition of the P-binding metal La in the form of a Flock (Fe(III)Cl) & Lock (La-modified bentonite; LMB) treatment in Lake De Kuil competes with Fe for P-binding. Accordingly, a large HCl-P pool was detected in our P fractionation analysis (Fig. 2) which can extract La-P (Dithmer et al. 2016; Reitzel et al. 2013), and P XANES analysis confirmed high contribution of HAp and the mineral monazite but not vivianite (Fig. 5B). In Lake Almind, microbial-driven denitrification coupled with Fe(II) oxidation, as described in Robertson and Thamdrup (2017) reduces direct Fe(II) availability but increases the probability for Fe(III)-P precipitation in the upper sediment. However, in the deeper anoxic sediment, vivianite was present, as confirmed by Bipy extraction and P XANES analysis (Figs. 2, 5B), likely a result of the transformation of buried Fe(III)-P phases. In Lake Ouderkerkerplas, oxygenation at the sediment surface prevented reducing conditions, which lowers the extent of Fe(II)-P precipitation and, thus, vivianite formation in the surface sediment. Finally, it should be noted that the applied Bipy extraction solution in KCl will always extract some Fe and P, since KCl is an electrolyte that can partially dissolve particle surface attached, ion exchangeable P (Li et al. 2012).

Impact of level of crystallinity on bipyridine extraction efficiency

In Lake Arendsee, the presence of highly crystalline vivianite was confirmed by XANES, XRD, and SEM–EDX at 36.5 cm sediment depth in our study (Fig. 6; Table 7; SI Sections G–I). Rothe et al. (2015) estimated that vivianite-P accounted for 45% of TP in deep sediment layers (26–48 cm depth) and reported predominant extraction in the NaOH fraction. In contrast, our Bipy results show a maximum of 16% vivianite-P at 36.5 cm sediment depth, with mostly the BD pool contributing to the Bipy extraction (Fig. 3). Given that our Fe and P XANES results better align with the estimates from Rothe et al. (2015) (Table 6), it suggests that Bipy only extracted approximately 26% of the total vivianite-P present.

Although the extraction behavior of vivianite is largely unknown, there are indications that the general extraction efficiency of minerals depends on their level of crystallinity and oxidative state (Rothe et al. 2014; Thompson et al. 2019). For instance, Rothe et al. (2015) found that a BD extraction almost fully dissolved freshly precipitated, amorphous vivianite, while only 14% of crystalline synthetic and natural vivianite was dissolved during the BD extraction and ~ 84% in the NaOH fraction as stronger metal bound P. In Lake Arendsee, in our study, mostly the BD pool contributed to Bipy, indicating that only the more amorphous vivianite-P was extracted by Bipy. Further, the sum of BD- and NaOH-iP in Lake Arendsee sediment was generally lower in our study compared to the findings of Rothe et al. (2015), even when using the Con protocol. It should be noted that we used 0.1 M instead of 1 M NaOH as used by Rothe et al. (2015) for the SPE, which could have affected the extraction efficiency.

On the other hand, smaller mineral crystal size can complicate direct mineral detection (Wang et al. (2021) and references therein). For example, crystalline vivianite was not found in GG using XRD, but SEM–EDX confirmed the presence of vivianite particles; however, they were smaller (100 μm) than in AS (150 μm), in which XRD confirmed the presence of crystalline vivianite. Similarly, in Lake Ørn, Bipy-iP concentrations were high throughout sediment depth (60–146 μmol P g^{-1} DW), while mainly the NaOH pool contributed to Bipy in this sediment (Figs. 4 and S5), suggesting that vivianite-P was present in a more crystalline form. Accordingly, small-sized (50 μm), blue-colored vivianite crystallites were identified at 19.5 cm sediment depth using SEM–EDX, but they were not visible in the XRD diffractogram (Fig. 6; Table 7; SI Section H). Additionally, LCF of P XANES spectra revealed a lower relative importance of vivianite-P compared to the extraction results (Fig. 5B; Table 6). This suggests that vivianite of smaller crystal size or more amorphous form can be extracted using Bipy, while successful direct spectroscopic mineral detection is impaired.

Hence, if the sample is highly crystalline, as found in AS, the Bipy extraction efficiency might be impaired and requires optimization of the extraction step, such as prolonged extraction time, higher extractant concentration, or additional extraction steps. Further research and validation are needed to confirm the potential negative effect of high crystallinity on the Bipy extraction efficiency and the effectiveness of suggested protocol optimizations. Moreover, it is strongly recommended that the Mod SPE protocol be combined with direct mineral detection methods, such as XRD and XANES and vice versa, as applied in this study. It helps to reveal and

address the potential limitations of each method with regard to the level of crystallinity.

Effect of sample oxidation, high OM and Fe content on bipyridine extraction efficiency, x-ray diffraction, and x-ray absorption near edge structure

Crystallinity is not the only factor influencing direct mineral detection. The sectioning and extraction were performed without a glovebox. Hence, sample oxidation during processing and analysis cannot be excluded. Since the study aimed to test the suitability of the Bipy modified protocol for routine applications and not all labs might be equipped with a glovebox, its use was suspended. During the extraction protocol, the first extraction step was performed with N_2-purged milli-Q to lower the oxygen exposure of the sample, while complexation of Fe(II) with Bipy was assumed to prevent further oxidation (Gu et al. 2016). Moreover, it was assumed that high organic matter content of the sample protects phases sensitive to oxidation. This has been reported for sulfur-associated with humic matter (Catrouillet et al. 2014). However, the Bipy extraction results seemed to be less affected by sample oxidation. In Rothe et al. 2016 it was stated that vivianite oxidation stabilizes around 50% Fe^{3+} of total Fe. It can be assumed that the outer Fe(III) shell protects the inner oriented remaining Fe(II) from oxidation. In the samples GG and ØN, SEM–EDX analysis confirmed the presence of surface-oxidized vivianite particles, but no crystalline vivianite was found using XRD. If the ratio between XANES estimates and Bipy is calculated from Table 6, it appears that the vivianite-P XANES results are approximately 35% and 43% of Bipy-P in these samples, respectively. Hence, sample oxidation impairs direct detection using XRD and XANES through changes in the mineral's structure and crystallinity, while the Bipy extraction efficiency appeared to be unaffected.

High OM% or excessive elemental contents (i.e., excessive Fe) can also complicate direct detection (Prietzel et al. 2016; Prietzel et al. 2007; Sjöström et al. 2019). In both Lakes Lyng and Ørn, a homogeneous depth distribution of Bipy-P with relatively high importance (33–51% and 22–37% of TP, respectively) throughout the upper 20 cm was found (Fig. 2). In contrast, comparatively low relative contributions of vivianite were found in LY and ØN by XANES (Fig. 5; Table 6) and vivianite was not detected using XRD. Likely, the high OM% ($\sim$ 60% in Lake Lyng, $\sim$ 25% in Lake Ørn, both with homogeneous depth distribution; Fig. S1), combined with high heterogeneity in Fe (Fe(II)/(III) proportion) and P speciation (Fig. 5), complicated direct mineral detection via XRD, XANES, Opt-Mic, or SEM–EDX. Similar observations were made for GG. Likewise, without pretreatment, for example, heavy-liquid separation, Rothe et al. (2014) could not detect crystalline vivianite via XRD in Lake Groβ Glienicker (OM $\sim$ 35%).

Although the Bipy extraction efficiency was seemingly not impaired by high OM%, indications were found that Bipy also partially mobilized labile organic phases (Figs. 2, 4, and S10). Changes in NRP and Humic-P, which are associated with labile organic P (Heinrich et al. 2022; Reitzel et al. 2007) were observed, while Fe XANES analysis confirmed minor removal of Fe-OM from the sample due to the Bipy extraction. Fe(II) in freshwater sediment can complex with humic substances, such as humic or fulvic acids, via (bidentate) interactions (Catrouillet et al. 2014; Daugherty et al. 2017). Daugherty et al. (2017) found that Bipy-like functional groups complexed 5–20% of the total Fe(II) in a solution with natural OM. Thus, OM-associated Fe(II) might be partially released during Bipy extraction, potentially mobilizing labile organic P, also resulting in overestimation of Bipy-Fe as reported in Table 6 or the minor mobilization of NRP and humic-P. However, the overall extent to which labile organic P was mobilized by Bipy in this study was generally < 10% of Sum_{ex} from the Mod protocol results and, thus, negligible. Nevertheless, we advise against applying wet oxidation on Bipy extractions before SRP analysis, as done in Lake Arendsee and Groβ Glienicker, to prevent the oxidation of potentially released labile organic P. Filtration of the extraction prior to P analysis can be considered.

Saturation of the Bipy compound due to the excessive Fe(II) contents in these sediments could be excluded based on the following calculations. According to Eq. 1 (*see* Introduction), 3 mol of Bipy are needed to complex with 1 mol of Fe(II). Hence, 0.2% Bipy would correspond to $\sim$ 320 μmol in 25 mL extractant solution, and thus, the maximum amount of complexed Fe(II) would be $\sim$ 107 μmol. Bipy-Fe in ØN corresponded to $\sim$ 64.5 μmol, which is only 60% of the maximum Fe(II) extraction capacity. Similarly, Bipy-Fe in LY was $\sim$ 39.3 μmol, which is only $\sim$ 37% of the maximum Fe(II) extraction capacity, indicating that Bipy was not saturated, even in these very Fe-rich sediments (Fig. S1). It should, however, be noted that the complexation of Bipy with divalent ions other than Fe^{2+}, such as Ca^{2+}, cannot be fully excluded. However, Li et al. 2012 and Gu et al. 2016 both exposed Ca-bound P reference materials to the Bipy extraction and found the extent of Ca-P mobilization to be negligible. Nevertheless, it can be recommended to investigate the release of other divalent metal ions during the Bipy extraction by component analysis of the extractions, especially in a highly heterogeneous sample such as freshwater sediment. For example, vivianite was absent in AL according to the LCF analysis of the Fe XANES, but P XANES reported rather high relative contributions of vivianite, and Bipy-iP levels were noticeable (Table 6). The high Fe content compared to the low P content (Figs. S1 and S2) could explain the lack of information for Fe-P speciation when using Fe XANES in this sediment and emphasizes the sensitivity of the XANES analysis to elemental contents. However, scorzalite was detected in this sample, indicating the release of both Fe(II) and Al by Bipy in this sediment.

These observations emphasize the complementary and quantitative power of the Bipy extraction in combination with

spectroscopic and x-ray absorption-based semi-quantitative methods in a highly heterogeneous, organic-rich sample. Conclusively, while the Bipy extraction seems to be impaired by high crystallinity, XRD analysis could exclude or confirm high crystallinity in a sample, while XANES is a helpful tool to get reliable information on the presence or absence of specific binding forms. In turn, while XRD and XANES are sensitive to sample oxidation, the content of the phase of interest, as well as high OM%, the Bipy extraction could compensate for those limitations and provide a reasonable estimate for vivianite-associated P also in organic- and Fe-rich freshwater sediments without oxygen exposure preventive measures. Alternatively, to improve solid-state analysis by XRD and XANES, a glovebox could be used to prevent oxygen exposure, or samples could be pretreated. For instance, organic matter could be removed by H_2O_2 treatment, or sample density separation may be applied to separate phases, as suggested in Rothe et al. (2014, 2015).

Non-linearity between Fe and P release in the bipyridine extraction

The observed molar Fe : P ratios in the Bipy extract (Table 4) were generally higher than the theoretical value of 1.5 reported for pure, crystalline vivianite (Al-Borno and Tomson 1994; Nriagu 1972). Additionally, Fe and P release in the Bipy extract was weakly correlated in most of the lakes (Table 5). This discrepancy could be attributed to: (1) the surface oxidation of vivianite (Roldán et al. 2002) during extraction, or (2) the release of Fe(II) species from Fe(II)-minerals other than vivianite present in the sediment, such as Fe(II) bound to clay minerals, siderite ($FeCO_3$), green rust ($[Fe^{2+}{}_4Fe^{3+}{}_2(OH^-)_{12}] \cdot [SO^{2-}{}_4 \cdot 2H_2O]$), magnetite ($Fe^{2+}Fe^{3+}{}_2O_4$), mixed Fe(II)-Ca-Mg carbonates, or humic substances as identified by Wallmann et al. (1993).

First, it cannot be ruled out that the vivianite in our samples was surface-oxidized, since no further oxygen exposure prevention measures were taken during sediment sampling, processing, and extraction. The presence of surface-oxidized vivianite was confirmed in the samples using SEM–EDX (Fig. 6; Table 7). Second, Gu et al. (2016) argued that most non-vivianite associated sedimentary Fe(II) was resistant to Bipy complexation. In our study, however, it appears that Bipy fully extracts vivianite-like bound P but probably extracts additional Fe(II) not associated with vivianite. For example, Fe concentrations in the Bipy extract from vivianite-poor sediments (AL and DK) were comparable to or higher than in vivianite-rich sediments (GG and AS) (Table 4) and Fe and P release were disproportional (Table 5). In Lake Ørn, especially the release of Fe(II)-OM might have caused this non-linearity (Table 3). In AL, the crystalline Fe(II)-Al-P phase scorzalite ($Fe^{2+}Al_2(PO_4)_2(OH)_2$) was identified using XRD in combination with SEM–EDX (Table 7; Fig. S9). Assuming that high crystallinity hinders P extraction by complexation (Thompson et al. 2019)—in LY, Bipy-iP was high despite the dominant presence of crystalline FeS—and that Fe(II)-P minerals other than vivianite account for only a small fraction of sedimentary TP, their contribution to Bipy-iP cannot be fully excluded but is likely minor.

Comments and recommendations

In this study, we demonstrate the suitability and reliability of the Bipy extraction inserted in a sequential P extraction protocol for estimating the importance of vivianite-like bound P in a range of freshwater sediments. The sum of extracted P pools was not affected by the insertion of the Bipy step (Figs. 3 and S5) and pre-edge analysis and LCF of Fe XANES spectra before and after the Bipy extraction confirmed the predominant removal of vivianite from the sediment (Fig. 2; Table 3). However, an underestimation of vivianite-P using Bipy was indicated in a sample with high crystallinity (AS) (Tables 6 and 7). On the contrary, in more heterogeneous samples with high Fe or OM content (ØN, LY, GG) the direct detection methods such as XRD and XANES were impaired and reported lower relative importance, while the Bipy extraction efficiency was not affected (Tables 6 and 7; Figs. 5 and S7).

Conclusively, it is strongly recommended to use the chemical extraction method in combination with direct detection methods whenever possible to guarantee reliable estimations and complementarity of methods. Moreover, it is recommended to further investigate the effect of crystallinity on the Bipy extraction efficiency, and to validate suggested protocol optimization strategies, such as extended extraction time, higher Bipy concentration, or additional extraction steps.

Finally, the non-linearity of the Fe and P release in the Bipy extract (Table 5) can be explained by the partial release of non-P bearing Fe(II) phases or ferrous P minerals other than vivianite, which include transformation and oxidation products such as metavivianite or other mixed valent Fe-P phases such as scorzalite as detected in AL. However, the environmental relevance of such Fe-P phases is rather low compared to vivianite in freshwater sediments. Further, the release of non-P bearing Fe(II) was found to be of minor concern since the Bipy extractant solution did not seem to be saturated even in Fe-rich samples and usually only P is quantified in the extractions to estimate the importance of the specific binding forms. It is, however, certainly of great interest to further investigate to what extent Bipy may complex with other divalent cations than Fe in freshwater sediment. For instance, by component analysis of the extraction solution.

In summary, the modified sequential P extraction protocol with a Bipy step inserted was found to deliver robust results if the separate quantification of Fe(II)-P and Fe(III)-P is an objective in a range of freshwater sediments with a focus on vivianite. The combination of the modified extraction protocol with the direct detection methods such as microscopy, XRD, and XANES is highly recommended, while the results of

the latter two could be improved using a glovebox or sample pretreatments.

Supporting information: (A) Depth profiles of total sedimentary Fe, P, Ca, Al, Mg, Mn, and organic matter (LOI %). (B) Patterns and motivations for sectioning of sediment cores. (C) Full schematic of the conventional and modified sequential P extraction protocol. (D) Synthesis protocol for reference materials (Fe(III)P & Vivianite). (E) Comparison of sum of extracted P pools between protocols. (F) Change of different P fractions (ΔFraction) in absolute concentration. (G) Fe and P XANES spectra of selected sediment samples and LCF. (H) XRD diffractograms. (I) Light microscopy and SEM–EDX (layered) images. (J) Change of NRP per fraction.

Author Contributions

Sina Haasler: Conceptualization, methodology, visualization, data—acquisition and analysis, writing—original draft preparation, editing, revision. Simon David Herzog: Supervision, methodology, visualization, data—acquisition and analysis, writing—reviewing and editing. David W. O'Connell: Supervision, methodology, data—acquisition, writing—reviewing. Worachart Wisawapipat: Methodology, data—acquisition and analysis, writing—reviewing. Qian Wang: Methodology, data—acquisition, writing—reviewing. Michael Hupfer: Methodology, writing—reviewing. Jéssica Papera: Data—acquisition, writing—reviewing. Theis Kragh: Supervision, writing—reviewing. Anna-Marie Klamt: Methodology, writing—reviewing. Kasper Reitzel: Conceptualization, supervision, writing—reviewing and editing.

Acknowledgments

Part of the research described in this paper was performed at the Canadian Light Source (CLS), a national research facility of the University of Saskatchewan, which is supported by the Canada Foundation for Innovation (CFI), the Natural Sciences and Engineering Research Council (NSERC), the Canadian Institutes of Health Research (CIHR), the Government of Saskatchewan, and the University of Saskatchewan. Additionally, part of the research was conducted at the Synchrotron Light Research Institute (SLRI) in Nakhon Ratchasima, Thailand. We are thankful to all technical and scientific staff from the CLS and SLRI for their professional support and advice. Especially Mohsen Shakuri from CLS, Wantana Klysubun at BL8 from SLRI, and Apinya Saentho from Kasetsart University, Thailand. We also acknowledge MAX IV Laboratory for time on Beamline BALDER under Proposal 20231797. Research conducted at MAX IV, a Swedish national user facility, is supported by the Swedish Research Council under contract 2018-07152, the Swedish Governmental Agency for Innovation Systems under contract 2018-04969, and Formas under contract 2019-02496. We are thankful to the technicians at the Department of Biology, Ecology group, SDU, particularly to Carina Lohmann for her assistance during the data collection at the SLRI in Thailand. The study involved two research guest stays at the Leibniz-Institute of Freshwater Ecology and Inland Fisheries (IGB) in Berlin, Germany, and at Wetsus—European Centre of Excellence for Sustainable Water Technology in Leeuwarden, the Netherlands. The hosting, including the provision of field and lab equipment, as well as valuable scientific input, is highly appreciated. The gues stays were funded by the European Union´s Horizon 2020 Research and Innovation program (RecaP project) under the Marie Sklodowska-Curie grant agreement No. 956454. Kasper Reitzel received support from the Poul Due Jensen/Grundfos Foundation under grant number (2020-068).

Conflicts of Interest

None declared.

References

Akinnawo, S. O. 2023. "Eutrophication: Causes, Consequences, Physical, Chemical and Biological Techniques for Mitigation Strategies." *Environmental Challenges* 12: 100733. https://doi.org/10.1016/j.envc.2023.100733.

Al-Borno, A., and M. B. Tomson. 1994. "The Temperature Dependence of the Solubility Product Constant of Vivianite." *Geochimica et Cosmochimica Acta* 58, no. 24: 5373–5378. https://doi.org/10.1016/0016-7037(94)90236-4.

Ansari, A. A., G. S. Singh, G. R. Lanza, and W. Rast. 2010. Eutrophication: Causes, Consequences and Control. Vol. 1. Springer.

Beckler, J. S., M. E. Jones, and M. Taillefert. 2015. "The Origin, Composition, and Reactivity of Dissolved Iron(III) Complexes in Coastal Organic- and Iron-Rich Sediments." *Geochimica et Cosmochimica Acta* 152: 72–88. https://doi.org/10.1016/j.gca.2014.12.017.

Boers, P., J. Van der Does, M. Quaak, J. Van der Vlugt, and P. Walker. 1992. "Fixation of Phosphorus in Lake Sediments Using Iron (III) Chloride: Experiences, Expectations." In Restoration and Recovery of Shallow Eutrophic Lake Ecosystems in The Netherlands: Proceedings of a conference held in Amsterdam, The Netherlands, 18–19 April 1991, edited by L. V. Liere and R. D Gulati, 211–212. Kluwer Academic Publishers.

Braga, B. B., T. R. A. de Carvalho, A. Brosinsky, S. Foerster, and P. H. A. Medeiros. 2019. "From Waste to Resource: Cost-Benefit Analysis of Reservoir Sediment Reuse for Soil Fertilization in a Semiarid Catchment." *Science of the Total Environment* 670: 158–169. https://doi.org/10.1016/j.scitotenv.2019.03.083.

Cakmak, E. K., M. Hartl, J. Kisser, and Z. Cetecioglu. 2022. "Phosphorus Mining From Eutrophic Marine Environment Towards a Blue Economy: The Role of Bio-Based Applications." *Water Research* 219: 118505. https://doi.org/10.1016/j.watres.2022.118505.

Canfield, D. E., Jr., M. Kiani, O. Tammeorg, P. Tammeorg, and T. J. Canfield. 2024. "Put the Land Back on the Land: A National Imperative." In Sediment Transport Research—Further Recent Advances. IntechOpen. https://doi.org/10.5772/intechopen.1004908.

Catrouillet, C., M. Davranche, A. Dia, et al. 2014. "Geochemical Modeling of Fe (II) Binding to Humic and Fulvic Acids." *Chemical Geology* 372: 109–118. https://doi.org/10.1016/j.chemgeo.2014.02.019.

Conley, D. J., H. W. Paerl, R. W. Howarth, et al. 2009. "Controlling Eutrophication: Nitrogen and Phosphorus." *Science* 323, no. 5917: 1014–1015. https://doi.org/10.1126/science.1167755.

Copetti, D., K. Finsterle, L. Marziali, et al. 2016. "Eutrophication Management in Surface Waters Using Lanthanum Modified Bentonite: A Review." *Water Research* 97: 162–174. https://doi.org/10.1016/j.watres.2015.11.056.

Cordell, D., J.-O. Drangert, and S. White. 2009. "The Story of Phosphorus: Global Food Security and Food for Thought." *Global Environmental Change* 19, no. 2: 292–305. https://doi.org/10.1016/j.gloenvcha.2008.10.009.

Crespi, J. M., C. Hart, C. C. Pudenz, L. L. Schulz, O. Wongpiyabovorn, and W. Zhang. 2022. An Examination of Recent Fertilizer Price Changes. Lowa State University. https://doi.org/10.1002/ev.20508.

Daugherty, E. E., B. Gilbert, P. S. Nico, and T. Borch. 2017. "Complexation and Redox Buffering of Iron (II) by Dissolved Organic Matter." *Environmental Science & Technology* 51, no. 19: 11096–11104. https://doi.org/10.1021/acs.est.7b03152.

Dillon, P. J., and L. A. Molot. 2024. "The Phosphorus Cycle." In Wetzel's Limnology, 359–425. Elsevier.

Dithmer, L., U. G. Nielsen, M. Lürling, et al. 2016. "Responses in Sediment Phosphorus and Lanthanum Concentrations and Composition Across 10 Lakes Following Applications of Lanthanum Modified Bentonite." *Water Research* 97: 101–110. https://doi.org/10.1016/j.watres.2016.02.011.

Evans, D., P. Johnes, and D. Lawrence. 2004. "Physico-Chemical Controls on Phosphorus Cycling in Two Lowland Streams. Part 2—the Sediment Phase." *Science of the Total Environment* 329, no. 1–3: 165–182. https://doi.org/10.1016/j.scitotenv.2004.02.023.

Fagel, N., L. Alleman, L. Granina, et al. 2005. "Vivianite Formation and Distribution in Lake Baikal Sediments." *Global and Planetary Change* 46, no. 1–4: 315–336. https://doi.org/10.1016/j.gloplacha.2004.09.022.

Findlay, D., H. Kling, H. Rönicke, and W. Findlay. 1998. "A Paleolimnological Study of Eutrophied Lake Arendsee (Germany)." *Journal of Paleolimnology* 19: 41–54. https://doi.org/10.1023/A:1007906611087.

Gu, C., T. Dam, S. C. Hart, et al. 2020. "Quantifying Uncertainties in Sequential Chemical Extraction of Soil Phosphorus Using XANES Spectroscopy." *Environmental Science & Technology* 54, no. 4: 2257–2267. https://doi.org/10.1021/es00058a023.

Gu, S., Y. Qian, Y. Jiao, Q. Li, G. Pinay, and G. Gruau. 2016. "An Innovative Approach for Sequential Extraction of Phosphorus in Sediments: Ferrous Iron P as an Independent P Fraction." *Water Research* 103: 352–361. https://doi.org/10.1016/j.watres.2016.07.058.

Haasler, S., T. Kragh, J. Magid, et al. 2024. "Recycling of Phosphorus From Dredged Lake Sediment: Importance of Iron-Bound Phosphates for Plant Growth." *Sustainable Environment* 10, no. 1: 2362503. https://doi.org/10.1080/27658511.2024.2362503.

Heinrich, L., J. Dietel, and M. Hupfer. 2022. "Sulphate Reduction Determines the Long-Term Effect of Iron Amendments on Phosphorus Retention in Lake Sediments." *Journal of Soils and Sediments* 22, no. 1: 316–333. https://doi.org/10.1007/s11368-021-03099-3.

Heinrich, L., M. Rothe, B. Braun, and M. Hupfer. 2021. "Transformation of Redox-Sensitive to Redox-Stable Iron-Bound Phosphorus in Anoxic Lake Sediments under Laboratory Conditions." *Water Research* 189: 116609. https://doi.org/10.1016/j.watres.2020.116609.

Heron, G., C. Crouzet, A. C. Bourg, and T. H. Christensen. 1994. "Speciation of Fe (II) and Fe (III) in Contaminated Aquifer Sediments Using Chemical Extraction Techniques." *Environmental Science & Technology* 28, no. 9: 1698–1705. https://pubs.acs.org/doi/pdf/10.1021/es00058a023.

Herzog, S. D., V. Mekelesh, M. Soares, U. Olsson, P. Persson, and E. S. Kritzberg. 2024. "Iron as a Precursor of Aggregation and Vector of Organic Carbon to Sediments in a Boreal Lake." *Biogeochemistry* 167, no. 12: 1533–1552. https://doi.org/10.1007/s10533-024-01184-6.

Hupfer, M., K. Reitzel, A. Kleeberg, and J. Lewandowski. 2016. "Long-Term Efficiency of Lake Restoration by Chemical Phosphorus Precipitation: Scenario Analysis With a Phosphorus Balance Model." *Water Research* 97: 153–161. https://doi.org/10.1016/j.watres.2015.06.052.

Huser, B. J., S. Egemose, H. Harper, et al. 2016. "Longevity and Effectiveness of Aluminum Addition to Reduce Sediment Phosphorus Release and Restore Lake Water Quality." *Water Research* 97: 122–132. https://doi.org/10.1016/j.watres.2015.06.051.

Ibendahl, G. 2022. *The Russia–Ukraine Conflict and the Effect on Fertilizer*. https://agmanager.info/sites/default/files/pdf/Ibendah_Fertizer_RussiaUkraine_03-08-22.pdf.

Jørgensen, C., H. S. Jensen, F. Ø. Andersen, S. Egemose, and K. Reitzel. 2011. "Occurrence of Orthophosphate Monoesters in Lake Sediments: Significance of Myo- and Scyllo-Inositol Hexakisphosphate." *Journal of Environmental Monitoring* 13, no. 8: 2328–2334. https://doi.org/10.1039/c1em10202h.

Karlsson, T., and P. Persson. 2012. "Complexes With Aquatic Organic Matter Suppress Hydrolysis and Precipitation of Fe (III)." *Chemical Geology* 322: 19–27. https://doi.org/10.1016/j.chemgeo.2012.06.003.

Karlsson, T., P. Persson, U. Skyllberg, C.-M. Morth, and R. Giesler. 2008. "Characterization of Iron (III) in Organic

Soils Using Extended X-Ray Absorption Fine Structure Spectroscopy." *Environmental Science & Technology* 42, no. 15: 5449–5454. https://doi.org/10.1021/es800322j.

Kiani, M., H. Raave, A. Simojoki, O. Tammeorg, and P. Tammeorg. 2021. "Recycling Lake Sediment to Agriculture: Effects on Plant Growth, Nutrient Availability, and Leaching." *Science of the Total Environment* 753: 141984. https://doi.org/10.1016/j.scitotenv.2020.141984.

Kiani, M., P. Tammeorg, J. Niemistö, A. Simojoki, and O. Tammeorg. 2020. "Internal Phosphorus Loading in a Small Shallow Lake: Response after Sediment Removal." *Science of the Total Environment* 725: 138279. https://doi.org/10.1016/j.scitotenv.2020.138279.

Kiani, M., J. Zrim, A. Simojoki, et al. 2023. "Recycling Eutrophic Lake Sediments into Grass Production: A Four-Year Field Experiment on Agronomical and Environmental Implications." *Science of the Total Environment* 870: 161881. https://doi.org/10.1016/j.scitotenv.2023.161881.

Kleeberg, A. 1997. "Interactions Between Benthic Phosphorus Release and Sulfur Cycling in Lake Scharmützelsee (Germany)." *Water, Air, and Soil Pollution* 99: 391–399. https://doi.org/10.1007/BF02406879.

Kleeberg, A., C. Herzog, and M. Hupfer. 2013. "Redox Sensitivity of Iron in Phosphorus Binding Does Not Impede Lake Restoration." *Water Research* 47, no. 3: 1491–1502. https://doi.org/10.1016/j.watres.2012.12.014.

Kubeneck, L. J., L. K. ThomasArrigo, K. A. Rothwell, R. Kaegi, and R. Kretzschmar. 2023. "Competitive Incorporation of Mn and Mg in Vivianite at Varying Salinity and Effects on Crystal Structure and Morphology." *Geochimica et Cosmochimica Acta* 346: 231–244. https://doi.org/10.1016/j.gca.2023.01.029.

Lenstra, W. K., M. Egger, N. A. Van Helmond, E. Kritzberg, D. J. Conley, and C. P. Slomp. 2018. "Large Variations in Iron Input to an Oligotrophic Baltic Sea Estuary: Impact on Sedimentary Phosphorus Burial." *Biogeosciences* 15, no. 22: 6979–6996. https://doi.org/10.5194/bg-15-6979-2018.

Li, Q., X. Wang, R. Bartlett, et al. 2012. "Ferrous Iron Phosphorus in Sediments: Development of a Quantification Method through 2,2′-Bipyridine Extraction." *Water Environment Research* 84, no. 11: 2037–2044. https://doi.org/10.2175/106143012X13373575830872.

Liu, J., X. Cheng, X. Qi, et al. 2018. "Recovery of Phosphate From Aqueous Solutions Via Vivianite Crystallization: Thermodynamics and Influence of pH." *Chemical Engineering Journal* 349: 37–46. https://doi.org/10.1016/j.cej.2018.05.064.

Lürling, M., F. Van Oosterhout, and E. Faassen. 2017. "Eutrophication and Warming Boost Cyanobacterial Biomass and Microcystins." *Toxins* 9, no. 2: 64. https://doi.org/10.3390/toxins9020064.

Murphy, J., and J. P. Riley. 1962. "A Modified Single Solution Method for the Determination of Phosphate in Natural Waters." *Analytica Chimica Acta* 27: 31–36. https://doi.org/10.1016/S0003-2670(00)88444-5.

Nriagu, J., and C. Dell. 1974. "Diagenetic Formation of Iron Phosphates in Recent Lake Sediments." *American Mineralogist: Journal of Earth and Planetary Materials* 59, no. 9–10: 934–946. https://doi.org/10.2138/am-1974-9-1010.

Nriagu, J. O. 1972. "Stability of Vivianite and Ion-Pair Formation in the System Fe_3 (PO_4) 2-$H_3PO_4H_3PO_4$-H_2O." *Geochimica et Cosmochimica Acta* 36, no. 4: 459–470. https://doi.org/10.1016/0016-7037(72)90035-X.

O'Connell, D. W., M. M. Jensen, R. Jakobsen, et al. 2015. "Vivianite Formation and Its Role in Phosphorus Retention in Lake Ørn, Denmark." *Chemical Geology* 409: 42–53. https://doi.org/10.1016/j.chemgeo.2015.05.002.

Palache, C., H. Berman, and C. Frondel. 1952. "Dana's System of Mineralogy." *Geologiska Föreningens i Stockholm Förhandlingar* 74, no. 2: 218–219. https://doi.org/10.1080/11035895209453366.

Paludan, C., and H. S. Jensen. 1995. "Sequential Extraction of Phosphorus in Freshwater Wetland and Lake Sediment: Significance of Humic Acids." *Wetlands* 15: 365–373. https://doi.org/10.1007/BF03160891.

Parsons, C. T., F. Rezanezhad, D. W. O'Connell, and P. Van Cappellen. 2017. "Sediment Phosphorus Speciation and Mobility Under Dynamic Redox Conditions." *Biogeosciences* 14, no. 14: 3585–3602. https://doi.org/10.5194/bg-14-3585-2017.

Phillips, E. J., and D. R. Lovley. 1987. "Determination of Fe (III) and Fe (II) in Oxalate Extracts of Sediment." *Soil Science Society of America Journal* 51, no. 4: 938–941. https://doi.org/10.2136/sssaj1987.03615995005100040021x.

Prietzel, J., G. Harrington, W. Häusler, K. Heister, F. Werner, and W. Klysubun. 2016. "Reference Spectra of Important Adsorbed Organic and Inorganic Phosphate Binding Forms for Soil P Speciation Using Synchrotron-Based K-Edge XANES Spectroscopy." *Journal of Synchrotron Radiation* 23, no. 2: 532–544. https://doi.org/10.1107/S1600577515023085.

Prietzel, J., J. Thieme, K. Eusterhues, and D. Eichert. 2007. "Iron Speciation in Soils and Soil Aggregates by Synchrotron-Based X-Ray Microspectroscopy (XANES, μ-XANES)." *European Journal of Soil Science* 58, no. 5: 1027–1041. https://doi.org/10.1111/j.1365-2389.2006.00882.x.

Prot, T., V. Nguyen, P. Wilfert, et al. 2019. "Magnetic Separation and Characterization of Vivianite From Digested Sewage Sludge." *Separation and Purification Technology* 224: 564–579. https://doi.org/10.1016/j.seppur.2019.05.057.

Reitzel, K. 2005. "Separation of Aluminum Bound Phosphate From Iron Bound Phosphate in Freshwater Sediments by a Sequential Extraction Procedure." In Phosphate in Sediments, edited by H. L. Golterman and L. Serrano, 109–117. Backhuys publishers.

Reitzel, K., J. Ahlgren, H. DeBrabandere, et al. 2007. "Degradation Rates of Organic Phosphorus in Lake

Sediment." *Biogeochemistry* 82: 15–28. https://doi.org/10.1007/s10533-006-9049-z.

Reitzel, K., J. Hansen, F. Ø. Andersen, K. S. Hansen, and H. S. Jensen. 2005. "Lake Restoration by Dosing Aluminum Relative to Mobile Phosphorus in the Sediment." *Environmental Science & Technology* 39, no. 11: 4134–4140. https://doi.org/10.1021/es0485964.

Reitzel, K., S. Lotter, M. Dubke, S. Egemose, H. S. Jensen, and F. Ø. Andersen. 2013. "Effects of Phoslock® Treatment and Chironomids on the Exchange of Nutrients Between Sediment and Water." *Hydrobiologia* 703: 189–202. https://doi.org/10.1007/s10750-012-1358-8.

Robertson, E. K., and B. Thamdrup. 2017. "The Fate of Nitrogen Is Linked to Iron (II) Availability in a Freshwater Lake Sediment." *Geochimica et Cosmochimica Acta* 205: 84–99. https://doi.org/10.1016/j.gca.2017.02.014.

Roldán, R., V. Barrón, and J. Torrent. 2002. "Experimental Alteration of Vivianite to Lepidocrocite in a Calcareous Medium." *Clay Minerals* 37, no. 4: 709–718. https://doi.org/10.1180/0009855023740072.

Rosenqvist, I. T. 1970. "Formation of Vivianite in Holocene Clay Sediments." *Lithos* 3, no. 4: 327–334. https://doi.org/10.1016/0024-4937(70)90039-3.

Rothe, M. 2016. "*Exploring Vivianite in Freshwater Sediments: From the Detection of Mineral Grains Towards the Understanding of their Occurrence*." Dissertation. Humboldt Universität zu Berlin, Berlin.

Rothe, M., T. Frederichs, M. Eder, A. Kleeberg, and M. Hupfer. 2014. "Evidence for Vivianite Formation and Its Contribution to Long-Term Phosphorus Retention in a Recent Lake Sediment: A Novel Analytical Approach." *Biogeosciences* 11, no. 18: 5169–5180. https://doi.org/10.5194/bg-11-5169-2014.

Rothe, M., A. Kleeberg, B. Grüneberg, K. Friese, M. Pérez-Mayo, and M. Hupfer. 2015. "Sedimentary Sulphur: Iron Ratio Indicates Vivianite Occurrence: A Study From Two Contrasting Freshwater Systems." *PLoS One* 10, no. 11: e0143737. https://doi.org/10.1371/journal.pone.0143737.

Rothe, M., A. Kleeberg, and M. Hupfer. 2016. "The Occurrence, Identification and Environmental Relevance of Vivianite in Waterlogged Soils and Aquatic Sediments." *Earth-Science Reviews* 158: 51–64. https://doi.org/10.1016/j.earscirev.2016.04.008.

Ruttenberg, K. C. 1992. "Development of a Sequential Extraction Method for Different Forms of Phosphorus in Marine Sediments." *Limnology and Oceanography* 37, no. 7: 1460–1482. https://doi.org/10.4319/lo.1992.37.7.1460.

Scholtysik, G., T. Goldhammer, H. W. Arz, M. Moros, R. Littke, and M. Hupfer. 2022. "Geochemical Focusing and Burial of Sedimentary Iron, Manganese, and Phosphorus During Lake Eutrophication." *Limnology and Oceanography* 67, no. 4: 768–783. https://doi.org/10.1002/lno.12019.

Sjöström, J. K., R. Bindler, T. Granberg, and M. E. Kylander. 2019. "Procedure for Organic Matter Removal From Peat Samples for XRD Mineral Analysis." *Wetlands* 39: 473–481. https://doi.org/10.1007/s13157-018-1093-7.

Smith, G. L., A. A. Reutovich, A. K. Srivastava, et al. 2021. "Complexation of Ferrous Ions by Ferrozine, 2,2′-Bipyridine and 1,10-Phenanthroline: Implication for the Quantification of Iron in Biological Systems." *Journal of Inorganic Biochemistry* 220: 111460. https://doi.org/10.1016/j.jinorgbio.2021.111460.

Smith, P., M. F. Cotrufo, C. Rumpel, et al. 2015. "Biogeochemical Cycles and Biodiversity as Key Drivers of Ecosystem Services Provided by Soils." *Soil* 1, no. 2: 665–685. https://doi.org/10.5194/soil-1-665-2015.

Smith, V. H. 2003. "Eutrophication of Freshwater and Coastal Marine Ecosystems a Global Problem." *Environmental Science and Pollution Research* 10: 126–139. https://doi.org/10.1065/espr2002.12.142.

Smith, V. H., and D. W. Schindler. 2009. "Eutrophication Science: Where Do We Go From Here?" *Trends in Ecology & Evolution* 24, no. 4: 201–207. https://doi.org/10.1016/j.tree.2008.11.009.

Søndergaard, M., J. P. Jensen, and E. Jeppesen. 1999. "Internal Phosphorus Loading in Shallow Danish Lakes." In Shallow Lakes'98. Developments in Hydrobiology, edited by N. Walz and B. Nixdorf, vol. 143, 145–152. Dordrecht: Springer. https://doi.org/10.1007/978-94-017-2986-4_15.

Sondergaard, M., P. J. Jensen, and E. Jeppesen. 2001. "Retention and Internal Loading of Phosphorus in Shallow, Eutrophic Lakes." *Scientific World Journal* 1: 427–442. https://doi.org/10.1100/tsw.2001.72.

Søndergaard, M., E. Jeppesen, and J. P. Jensen. 2000. "Hypolimnetic Nitrate Treatment to Reduce Internal Phosphorus Loading in a Stratified Lake." *Lake and Reservoir Management* 16, no. 3: 195–204. https://doi.org/10.1080/07438140009353963.

Søndergaard, M., E. Jeppesen, T. L. Lauridsen, et al. 2007. "Lake Restoration: Successes, Failures and Long-Term Effects." *Journal of Applied Ecology* 44, no. 6: 1095–1105. https://doi.org/10.1111/j.1365-2664.2007.01363.x.

Stroom, J., T. Pelsma, J. Beemster, J. Stoffels, and C. Hogenes. 2010. Ouderkerkerplas: systeemanalyse en onderzoek flexibel peil. Amsterdam: Waternet.

Tammeorg, O., I. Chorus, B. Spears, et al. 2024. "Sustainable Lake Restoration: From Challenges to Solutions." *WIREs Water* 11, no. 2: e1689. https://doi.org/10.1002/wat2.1689.

Thompson, J., S. W. Poulton, R. Guilbaud, K. A. Doyle, S. Reid, and M. D. Krom. 2019. "Development of a Modified SEDEX Phosphorus Speciation Method for Ancient Rocks and Modern Iron-Rich Sediments." *Chemical Geology* 524: 383–393. https://doi.org/10.1016/j.chemgeo.2019.07.003.

Tu, L., M. Moyle, J. F. Boyle, et al. 2023. "Anthropogenic Modification of Phosphorus Sequestration in Lake Sediments During the Holocene: A Global Perspective." *Global and Planetary Change* 229: 104222. https://doi.org/10.1016/j.gloplacha.2023.104222.

Vuillemin, A., A. Friese, R. Wirth, et al. 2020. "Vivianite Formation in Ferruginous Sediments From Lake Towuti, Indonesia." *Biogeosciences* 17, no. 7: 1955–1973. https://doi.org/10.5194/bg-17-1955-2020.

Waajen, G., F. van Oosterhout, G. Douglas, and M. Lürling. 2016. "Management of Eutrophication in Lake De Kuil (The Netherlands) Using Combined Flocculant–Lanthanum Modified Bentonite Treatment." *Water Research* 97: 83–95. https://doi.org/10.1016/j.watres.2015.11.034.

Waajen, G. W., E. J. Faassen, and M. Lürling. 2014. "Eutrophic Urban Ponds Suffer From Cyanobacterial Blooms: Dutch Examples." *Environmental Science and Pollution Research* 21: 9983–9994. https://doi.org/10.1007/s11356-014-2948-y.

Wallmann, K., K. Hennies, I. König, W. Petersen, and H.-D. Knauth. 1993. "New Procedure for Determining Reactive Fe (III) and Fe (II) Minerals in Sediments." *Limnology and Oceanography* 38, no. 8: 1803–1812. https://doi.org/10.4319/lo.1993.38.8.1803.

Wang, C., Y. Zhang, H. Li, and R. J. Morrison. 2013. "Sequential Extraction Procedures for the Determination of Phosphorus Forms in Sediment." *Limnology* 14: 147–157. https://doi.org/10.1007/s10201-012-0397-1.

Wang, Q., T.-H. Kim, K. Reitzel, N. Almind-Jørgensen, and U. G. Nielsen. 2021. "Quantitative Determination of Vivianite in Sewage Sludge by a Phosphate Extraction Protocol Validated by PXRD, SEM-EDS, and 31P NMR Spectroscopy Towards Efficient Vivianite Recovery." *Water Research* 202: 117411. https://doi.org/10.1016/j.watres.2021.117411.

Webb, S. 2005. "SIXpack: A Graphical User Interface for XAS Analysis Using IFEFFIT." *Physica Scripta* 2005, no. T115: 1011. https://doi.org/10.1238/Physica.Topical.115a01011.

Welch, E. B., and G. D. Cooke. 2005. "Internal Phosphorus Loading in Shallow Lakes: Importance and Control." *Lake and Reservoir Management* 21, no. 2: 209–217. https://doi.org/10.1080/07438140509354430.

Weng, L., W. H. Van Riemsdijk, and T. Hiemstra. 2012. "Factors Controlling Phosphate Interaction With Iron Oxides." *Journal of Environmental Quality* 41, no. 3: 628–635. https://doi.org/10.2134/jeq2011.0250.

Wijdeveld, W., T. Prot, G. Sudintas, P. Kuntke, L. Korving, and M. Van Loosdrecht. 2022. "Pilot-Scale Magnetic Recovery of Vivianite From Digested Sewage Sludge." *Water Research* 212: 118131. https://doi.org/10.1016/j.watres.2022.118131.

Wilke, M., F. Farges, P.-E. Petit, G. E. Brown Jr., and F. Martin. 2001. "Oxidation State and Coordination of Fe in Minerals: An Fe K-XANES Spectroscopic Study." *American Mineralogist* 86, no. 5–6: 714–730. https://doi.org/10.2138/am-2001-5-612.

Wojdyr, M. 2010. "Fityk: A General-Purpose Peak Fitting Program." *Journal of Applied Crystallography* 43, no. 5: 1126–1128. https://doi.org/10.1107/S0021889810030499.

Wolter, K.-D. 2010. "Restoration of Eutrophic Lakes by Phosphorus Precipitation, With a Case Study on Lake Gross-Glienicker." In Restoration of Lakes, Streams, Floodplains, and Bogs in Europe. Wetlands: Ecology, Conservation and Management, edited by M. Eiseltová, vol. 3, 85–99. Dordrecht: Springer. https://doi.org/10.1007/978-90-481-9265-6_7.

Yin, H., M. Zhang, P. Yin, and J. Li. 2022. "Characterization of Internal Phosphorus Loading in the Sediment of a Large Eutrophic Lake (Lake Taihu, China)." *Water Research* 225: 119125. https://doi.org/10.1016/j.watres.2022.119125.

Yuan, H., Z. Tai, Q. Li, and E. Liu. 2020. "In-Situ, High-Resolution Evidence From Water-Sediment Interface for Significant Role of Iron Bound Phosphorus in Eutrophic Lake." *Science of the Total Environment* 706: 136040. https://doi.org/10.1016/j.scitotenv.2019.136040.

Zhang, J., Z. Chen, Y. Liu, W. Wei, and B.-J. Ni. 2022. "Phosphorus Recovery From Wastewater and Sewage Sludge as Vivianite." *Journal of Cleaner Production* 370: 133439. https://doi.org/10.1016/j.jclepro.2022.133439.

Supporting Information

Additional Supporting Information may be found in the online version of this article.

Submitted 07 November 2024
Revised 23 July 2025
Accepted 24 July 2025